T.C.
DOKUZ EYLUL UNIVERSITY
IZMIR INTERNATIONAL
BIOMEDICINE AND GENOME
INSTITUTE

HIGH INCIDENCE OF MITOCHONDRIAL ETIOLOGY UNDERLYING NEUROGENETIC DISORDERS IN CONSANGUINEOUS TURKISH FAMILIES

ECE SONMEZLER

MOLECULAR BIOLOGY AND GENETICS

MASTER THESIS

IZMIR-2019

Thesis code: DEU.HSI.MSc/20168500008

T.C.
DOKUZ EYLUL UNIVERSITY
IZMIR INTERNATIONAL
BIOMEDICINE AND GENOME
INSTITUTE

HIGH INCIDENCE OF MITOCHONDRIAL ETIOLOGY UNDERLYING NEUROGENETIC DISORDERS IN CONSANGUINEOUS TURKISH FAMILIES

MOLECULAR BIOLOGY AND GENETICS

MASTER THESIS

ECE SONMEZLER

Assist. Prof. Yavuz OKTAY

(This research project was supported by TUBITAK. Project No.216S771)

Thesis code: DEU.HSI.MSc/2016850008

T.C.

DOKUZ EYLÜL ÜNİVERSİTESİ
İZMİR ULUSLARARASI BİYOTIP VE GENOM ENSTİTÜSÜ MÜDÜRLÜĞÜ

YÜKSEK LİSANS TEZ ONAY FORMU

Dokuz Eylül Üniversitesi İzmir Uluslararası Biyotıp ve Genom Enstitüsü Genom Bilimleri ve Moleküler Biyoteknoloji Anabilim Dalı, Moleküler Biyoloji ve Genetik Yüksek Lisans Programı öğrencisi 2016850008 numaralı Ece SÖNMEZLER, **"HIGH INCIDENCE OF MITOCHONDRIAL ETIOLOGY UNDERLYING NEUROGENETIC DISORDERS IN CONSANGUINEOUS TURKISH FAMILIES"** konulu Yüksek Lisans tezini 28.06.2019 tarihinde başarılı olarak tamamlamıştır.

BAŞKAN
Dr. Öğr. Üyesi Yavuz OKTAY
DEÜ İzmir Uluslararası Biyotıp ve Genom Enstitüsü
Genom Bilimleri ve Moleküler Biyoteknoloji Anabilim Dalı

JÜRİ ÜYESİ
Prof.Dr. Ayşe Semra HIZ
DEÜ Tıp Fakültesi
Çocuk Sağlığı ve Hastalıkları Ana Bilim Dalı

JÜRİ ÜYESİ
Prof.Dr. Hüseyin ONAY
Ege Üniversitesi Tıp Fakültesi
Tıbbi Genetik Ana Bilim Dalı

TABLE OF CONTENTS

LIST OF FIGURES

LIST OF TABLES

ABBREVIATIONS

ATP : Adenosine Triphosphate

BN : Blue-Native

CACNB4 : Calcium Voltage-Gated Channel Auxiliary Subunit Beta 4

CADD : Combined Annotation Dependent Depletion

ChIP-seq : Chromatin Immunoprecipitation Sequencing

CLP1 : Cleavage and Polyadenylation Factor I Subunit

CMT : Charcot Marie Tooth

CNV : Copy Number Variation

CONSEQUITUR : Consanguineous Neurogenetic Sequencing in Turkey

ExAC : Exome Aggregation Consortium

gnomAD : Genome Aggregation Database

GSS : Glutathione Synthetase

HPO : Human Phenotype Ontology

Indel : Insertion-deletion

iNPC : Induced neuronal progenitor cells

LGMD2K : Limb-girdle muscle dystrophy type 2K

MCCC2 : Methylcrotonoyl-CoA carboxylase 2

NGS : Next Generation Sequencing

OCLN : Occludin

OXPHOS : Oxidative Phosphorylation

PAGE : Polyacrylamide Gel Electrophoresis

PTPMT1 : Protein Tyrosine Phosphatase Mitochondrial 1

POMT1 : Protein O-mannosyltransferase 1

PRKCG : Protein Kinase C Gamma

RD : Rare Disease

SDS : Sodium Dodecyl Sulfate

SLC26A3 : Solute Carrier Family 26 Member 3

SV : Structural Variant

SNP : Single Nucleotide Polymorphism

SO : Sequence Ontology

SNV : Single Nucleotide Variant

TBS : Tris Buffered Saline

TLK2 : Tousled Like Kinase 2

TSEN : tRNA-splicing endonuclease subunits

WES : Whole Exome Sequencing

WGS : Whole Genome Sequencing

NCBI : National Center for Biotechnology Information

SIFT : The Sorting Intolerant from Tolerant

PP2 : Polymorphism Phenotyping v2

WWS : Walker-Warburg syndrome

TACO1 : Translational Activator of Cytochrome C Oxidase I

SAMHD1 : SAM and HD Domain Containing Deoxynucleoside Triphosphate

ACKNOWLEDGEMENTS

First, I would like to express my sincere appreciation to my supervisor Dr. Yavuz OKTAY for his continuous support, guidance and encouragement during last three years. Having a chance to complete my Master's degree in Oktay Lab helped me to become improved both personally and scientifically. I'm very grateful for his valuable criticism and the opportunities he has offered me during my study.

I would like to extend my special thanks to Prof. Dr. Ayşe Semra HIZ and her team for their cooperation and extremely valuable criticism through this work. I am very grateful for her attentive personality and superior effort in leading the project.

I also would like to thank other valuable clinicians Prof. Dr. Serdal Güngör and Prof. Dr. Ahmet Yaramış for recruiting patients. Additionally, I would like to thank all families included in this study for their cooperation.

I greatly appreciate all Oktay Lab members: Burcu Ekinci, Tutku Yaraş, Kaan Okay, Aykut Kuruoğlu, Fadime Öztoprak and Ebru Diler for their friendship and wonderful fun times. They all were like sisters and brothers for me.

I am thankful to my lovely friends Yağmur Toktay, Esra Katkat and Mehmet Ergüven for their good energy and great friendship.

I am also very grateful to my beloved Ahmet Salih Adalı for his love and endless support in every moment of last six years.

Finally, I would like to express my deepest gratitude and appreciation to my dearest family, my mother Hülya Sönmezler, my father Mahmut Sönmezler, my sister Özge Sönmezler Duran, my brother Muzaffer Duran and my grandparents for being always there to support me in all my decisions.

June 2019 Ece SONMEZLER

HIGH INCIDENCE OF MITOCHONDRIAL ETIOLOGY UNDERLYING NEUROGENETIC DISORDERS IN CONSANGUINEOUS TURKISH FAMILIES

Ece Sonmezler, Dokuz Eylul University Izmir International Biomedicine and Genome Institute, ece.sonmezler@msfr.ibg.edu.tr

ABSTRACT

Neurogenetic diseases are conditions that affect the brain, spinal cord, nerves and muscles. Neurogenetic diseases can be categorized as single gene disorders with autosomal, X-linked or mitochondrial inheritance, polygenic disorders, multifactorial disorders and disorders caused by inherited or de novo chromosomal abnormalities. Due to complicated clinical features and genetic heterogeneity of them and limitations in traditional diagnostic approaches, neurogenetic diseases are difficult to diagnose.

Advances in the next-generation sequencing (NGS) technologies facilitate the molecular diagnosis and the discovery of novel disease genes and variants. Today, high-throughput, cost and time-effective whole exome sequencing (WES) is mostly preferable strategy used in diagnostic process of genetic diseases including neurogenetic diseases.

In the frame of this project, 191 consanguineous families with childhood neurogenetic disorders were recruited and deeply phenotyped. To date, 138 of them underwent WES and causative genetic defect for 79 of them were identified with diagnostic yield of 57%. Among identified genes, 28 of them are known variants and 32 of them are novel candidate variants in known disease genes which are already associated with neurogenetic diseases and 15 of them are novel candidate genes. Importantly, mitochondrial function associated genes were higher than expected.

By obtaining a diagnostic yield of 57% in such a large cohort, we showed the diagnostic utility of WES in neurogenetic diseases, identified novel candidate disease genes and variants by explaining genotype-phenotype relations in detail and provided genetic counseling and disease-specific therapies for some of the families.

Keywords: NGS, WES, neurogenetic diseases, mitochondrial, consanguineous families

TÜRKİYE'DE AKRABA EVLİLİĞİNE BAĞLI NÖROGENETİK HASTALIKLARIN TEMELİNDE YATAN MİTOKONDRİYAL ETİYOLOJİNİN SIKLIĞI

Ece Sönmezler, Dokuz Eylül Üniversitesi İzmir Uluslararası Biyotıp ve Genom Enstitüsü, ece.sonmezler@msfr.ibg.edu.tr

ÖZET

Nörogenetik hastalıklar beyin, omurilik, kas ve periferik sinirleri etkileyen hastalıklardır. Nörogenetik hastalıklar otozomal, X'e bağlı ya da mitokondriyal kalıtım gösteren tek gen hastalıkları, poligenik, multifaktöriyel kalıtımlı hastalıklar ve de novo ya da kalıtılan kromozomal bozukluklar olarak gruplandırılırlar. Karmaşık klinik bulgular, genetik heterojenite ve geleneksel tanı yöntemlerindeki sınırlamalar nedeniyle nörogenetik hastalıkların teşhisinde bir takım zorluklar yaşanmaktadır.

Yeni nesil dizileme (NGS) teknolojilerindeki gelişmeler, moleküler tanılamayı, yeni hastalık genlerinin ve varyantlarının keşfedilmesini kolaylaştırmaktadır. Bugün, yüksek verimli, düşük maliyetli ve zaman kazandıran tüm ekzom dizileme (WES) yöntemi, nörogenetik hastalıklar da dahil olmak üzere genetik hastalıkların tanı sürecinde çoğunlukla tercih edilen bir stratejidir.

Bu proje çerçevesinde, çocukluk çağı nörogenetik bozukluk bulunduran 191 akraba aile kayıtlandı ve etkilenmiş aile bireylerinin kapsamlı fenotiplemesi yapıldı. Bugüne kadar çalışmamız kapsamında 138 aileye WES uygulanmış olup ve toplamda 79'u için moleküler tanı %57 tanısal verim ile tespit edildi. Tanımlanmış genler içinde 32 tanesi nörogenetik hastalıklar ile ilişkilendirilmiş genlerde bulunan yeni aday varyantlar, 28 tanesi nörogenetik hastalıklar ile ilişkilendirilmiş genlerde bulunan bilinen varyantlar ve 15 tanesi yeni aday genler olarak tespit edildi. Mitokondri ile ilişkili genler beklenenden daha yüksek oranda tespit edildi.

Böylesine büyük bir kohortta %57 tanısal verim elde edilerek, WES'in nörogenetik hastalıklarda tanısal önemi gösterildi, genotip-fenotip ilişkileri ayrıntılı olarak açıklanarak yeni hastalık genleri ve varyantları belirlendi, bazı ailelere genetik danışmanlık ve hastalığa özgü tedaviler sağlandı.

Anahtar kelimeler: NGS, WES, nörogenetik hastalıklar, mitokondriyal, akraba aileler

1.INTRODUCTION

1.1 Neurogenetic Disorders

Neurogenetic disorders result from the dysfunction of peripheral or central nervous system. Nerves, muscles, spinal cord and the brain are mainly affected by these conditions (Faghihi, Mottagui-Tabar, & Wahlestedt, 2004). The normal function of the central nervous system depends on thousands of genes performing correctly. Thus, a large proportion of genetic disorders affect nervous system functions by different mechanisms.

Neurogenetic disorders can be caused by chromosomal abnormalities such as structural rearrangements, chromosomal insertions and deletions that impair cell function. Most of them are not inherited and they frequently involve mental retardation, epilepsy, and dysmorphic characteristics. Trisomy 21, Turner syndrome, Cri du chat syndrome (5p-) and Miller-Dieker syndrome (17p-) are examples for chromosomal neurogenetic disorders (Toft, 2014).

Mendelian neurological disorders referred to as monogenic neurological disorders caused by a single gene mutation in nuclear DNA. They can be inherited in an autosomal dominant pattern such as Huntington's disease, hereditary neuropathy and ataxias, autosomal recessive pattern such as some cerebellar ataxias, Neimann Pick disease and Tay-Sach's disease and X-linked dominant or recessive pattern such as Charcot-Marie-Tooth disease and Duchenne's muscular dystrophy.

Mitochondrial DNA mutations that are inherited from the mother are also common causes of the development of neurogenetic conditions such as mitochondrial encephalomyopathy, lactic acidosis, and stroke-like episodes (MELAS) and Myoclonic epilepsy with ragged-red fibers (MERRF).

Neurogenetic disorders can also be polygenic or multifactorial with the additive effects of more than one gene and environmental factors (Bird, 2005).

In children, hereditary neurological disorders are relatively frequent compared to adulthood. For the choice of genetic testing, evaluation of genetic test results and genetic consultation, it is important to comprehensively recognize clinical manifestations of hereditary neurological disorders. Improvements in next generation sequencing (NGS) technologies have made it possible to discover genetic causes of hereditary neurological disorders significantly, as well as reduce the challenge of applying genetic evaluation for clinicians. So, combination of clinical data and advanced technologies will improve the performance of genetic testing in

clinical practice and the understanding of genetic basis of neurogenetic disorders (Huang Y, Yu S, Wu Z, 2014)

1.2 Consanguineous Populations and Genetic Studies

Union between two related individuals who are second cousin or closer is defined as a consanguineous marriage. In different parts of the world, the rate of consanguineous marriage relies on various factors such as education, religious beliefs, local culture and socio-economic status. Consanguineous marriages have higher rates in Middle Eastern, West Asian and North African populations with 20-50% (Hamamy, 2012).

Studying with consanguineous parents' offspring is important for genetic studies because offspring from consanguineous unions shows high level of homozygosity for the loci that are inherited from the common ancestor and responsible for the development of mostly rare autosomal recessive disorders (Erzurumluoglu, Shihab, Rodriguez, Gaunt, & Day, 2016).

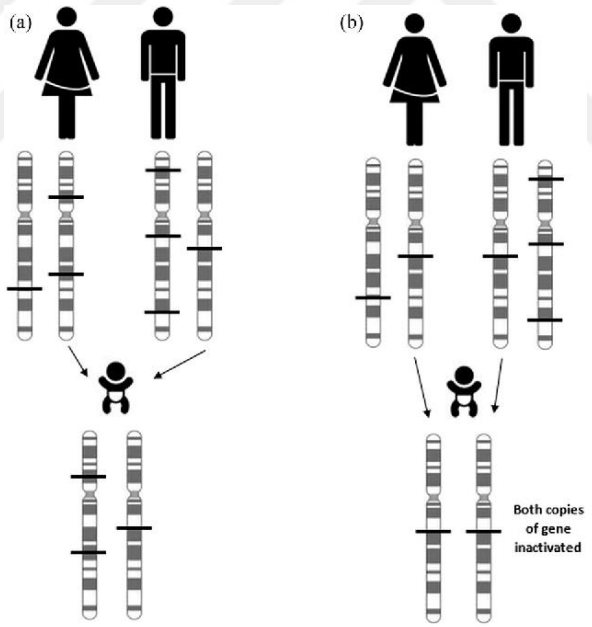

Figure 1.1 Comparison of non-consanguineous (a) and consanguineous unions (b) for leading homozygous loss of function mutations. Due to having common ancestor and higher homozygosity level, offspring of consanguineous couples has higher possibility of carrying homozygous loss of function mutations when compared with offspring of non-consanguineous couples (Erzurumluoglu et al., 2016).

1.3 Mitochondrial Etiology of Neurogenetic Disorders

Nervous system contains the most energy requiring cells of the body and neuronal activity highly depends on the energy from the mitochondrial oxidative phosphorylation (OXPHOS) system. Mitochondria produce the energy potential through the respiratory complexes I to V and generate energy in the form of ATP to sustain different biological processes (Giachin, Bouverot, Acajjaoui, & Pantalone, 2016). In many human diseases, dysfunction of mitochondria results in altered cellular redox equilibrium, altered bioenergetics and cellular dynamics. Thus, even small changes in the production of mitochondrial energy will have a preferential effect on the nervous system's most energy demanding organs due to their high ATP requirement for functioning (Kumar, 2016).

1.3.1 Mitochondrion Structure and Function

Mitochondria are the vital double membrane organelles which are known as "powerhouse of the cell". In eukaryotes, mitochondria provide the energy for cellular activities by carrying electron-transport processes to supply most of the cell's ATP (Kumar, 2016). According to historical endosymbiont hypothesis, mitochondrion has evolved from bacterial progenitor which is engulfed by host eukaryotic cell (Gray, 2012). As a proof of its bacterial origin, mitochondria have their own circular, double stranded, ~16kb long DNA which is inherited maternally in the oocyte cytoplasm. Mitochondrial DNA (mtDNA) with 37 genes encodes 13 subunits of oxidative phosphorylation (OXPHOS) components, 22 tRNAs and 2 rRNAs. For the proper functioning of mitochondrial OXPHOS complexes, mitoproteome also needs to ~1300 proteins encoded by nuclear genome (Alston, Rocha, Lax, Turnbull, & Taylor, 2017).

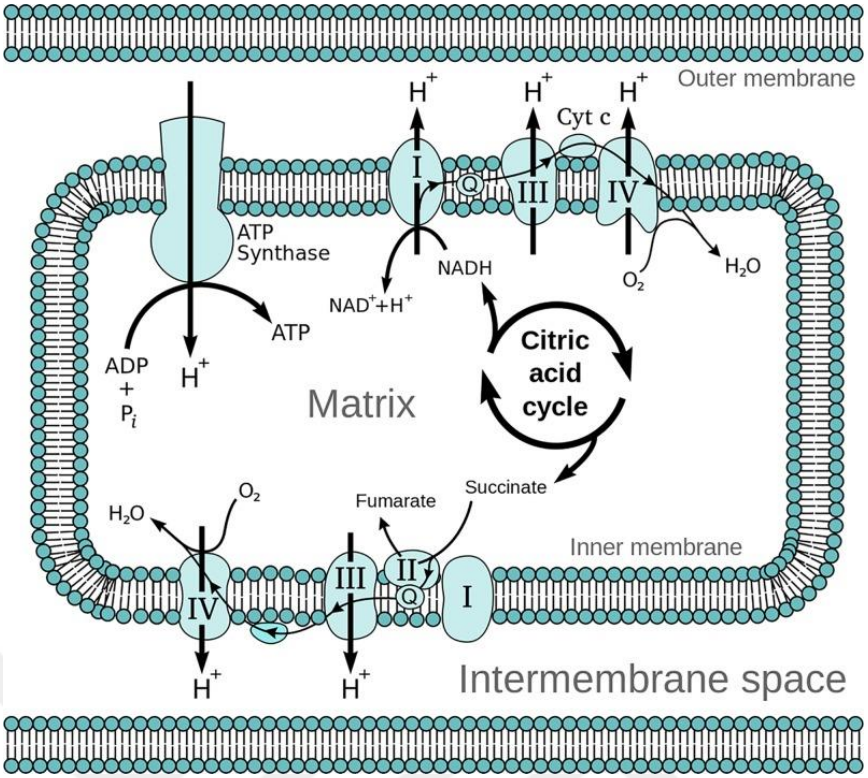

Figure 2.2 Electron transport chain (ETC). Transportation of electrons through the OXPHOS complexes to synthesize ATP (Jackson, Marks, May, & Wilson, 2018)**.**

1.3.2 Mitochondrial Complexes and Respiratory Chain Defects

Mitochondrial respiratory chain contains five complexes. Electron transportation initiating complex I (NADH: ubiquinone oxidoreductase) is the largest multi-subunit enzyme that is composed of 45 subunits and 7 of them are mitochondrial DNA encoded. Evolutionary conserved and functionally essential 14 core subunits include mitochondrial DNA and nuclear DNA encoded components together. These "core subunits" are sufficient for catalysis of energy transducing reactions and remaining 31 subunits are known as "accessory subunits" with mostly unknown function (Stroud et al., 2016).

Isolated complex I (Human NADH-Ubiquinone Oxidoreductase) deficiency is one of the most common causes of oxidative phosphorylation disorders and it accounts for ~30% of total mitochondrial cases (Fassone & Rahman, 2012).

Isolated complex I deficiency shows great heterogeneity both clinically and genetically. Complex I deficiency can be resulted from mutations in mitochondrial genes or nuclear genes. Most common clinical presentations are Leigh syndrome, cardiomyopathy, fatal infantile lactic

acidosis, cataracts, leukoencephalopathy and encephalomyopathy (Loeffen, Smeitink, Trijbels, Janssen, & Triepels, 2000).

Complex I deficiency can be caused by mutations in core subunit, supernumerary subunit and assembly factor encoding genes. Core subunits include 14 different subunits which are essential for catalytic activity. Seven of them are encoded by mitochondrial DNA (ND1, ND2, ND3, ND4, ND4L, ND5 and ND6) and remaining seven subunits are encoded by nuclear DNA (NDUFV1, NDUFV2, NDUFS1, NDUFS2, NDUFS3, NDUFS7 and NDUFS8). In addition to core subunit encoding genes, pathogenic mutations that cause complex I deficiency were also shown in genes (NDUFS4, NDUFS6, NDUFA1, NDUFA2, NDUFA10, NDUFA11 and NDUFA12) encoding supernumerary subunits with mostly unknown function (Mimaki, Wang, Mckenzie, Thorburn, & Ryan, 2012). There are also complex I deficiency linked various assembly factors (NDUFAF1, NDUFAF2, NDUFAF3, NDUFAF4, C20ORF7, C8ORF38, NUBPL, FOXRED1, ACAD9, TIMMDCI, ECSIT, ATP5SL etc.) which have functions in biogenesis of subunits, their assembly and stability (Formosa, Dibley, Stroud, & Ryan, 2018).

Mitochondrial complex II (succinate dehydrogenase-SDH or succinate:ubiquinone oxidoreductase-SQR) is a mitochondrial respiratory chain component which has role in both oxidative phosphorylation (OXPHOS) and tricarboxylic acid (TCA) cycle. Complex II deficiency is a rarely seen type of deficiency among oxidative phosphorylation disorders. Human mitochondrial complex II is formed from four nuclear DNA encoded subunits (SDHA, SDHB, SDHC and SDHD) which form heterotetramer and several assembly factors (SDHAF1, SDHAF2, SDHAF3 and SDHAF4) (Bezawork-Geleta, Rohlena, Dong, Pacak, & Neuzil, 2017). Most common clinical presentations of complex II deficiency are reported as Leigh syndrome, encephalomyopathy and tumor susceptibility such as paragangliomas, gastrointestinal stromal tumors, renal cell carcinoma (Ardissone et al., 2015).

Mitochondrial complex III (bc1 complex or ubiquinol cytochrome c reductase) is a central component of the electron transport chain with coenzyme Q oxidation and cytochrome c reduction functions. Complex III is a dimeric protein with 11 subunits and only cytochrome b subunit is encoded by mtDNA. Remaining 10 subunits are encoded by nuclear DNA. Complex III (cytochrome bc1) deficiency is one of the least frequently diagnosed types of OXPHOS deficiencies. Mutations that have been associated to complex III deficiency are structural subunit encoding nuclar UQCRB, UQCRQ, UQCRC2, CYC1 (cytochrome c1) genes, assembly factor encoding nuclear TTC19, LYRM7, UQCC2, UQCC3, BCS1L genes and only

mitochondrial DNA encoded MT-CYB (cytochrome b) gene (Fernández-Vizarra & Zeviani, 2015). Complex III deficiency cause variable clinical findings mostly including encephalopathy, renal and liver dysfunction, lactic acidosis, myopathy and cardiomyopathy (Bénit, Lebon, & Rustin, 2008).

Mammalian complex IV, also known as cytochrome c oxidase (COX), is a 200kDa multisubunit enzyme which has a role in the final step of the electron transport chain. Mitochondrial complex IV catalyzes the cytochrome c oxidation and four electrons from cytochrome c oxidation are used to convert molecular oxygen to water. Then, electrons taken from the mitochondrial matrix is translocated across the inner mitochondrial membrane to generate electrochemical gradient to synthesize ATP in further steps (Signes & Fernandez-Vizarra, 2018). Mammalian complex IV consists of 13 subunits. Catalytic core forming three largest subunits are encoded by mtDNA and structural integrity maintaining, remaining 10 subunits are encoded by nuclear DNA (McKenzie, Thorburn, Lazarou, Smith, & Ryan, 2009).

To date, mutations in structural subunit encoding COX4I2, COX7B, COX6B1 and ancillary factor encoding SURF1, SCO1, SCO2, COX10, COX15, LRPPRC and TACO1 genes have been associated with complex IV deficiency. Mostly related clinical phenotypes are encephalomyopathy, Leigh syndrome, cardiomyopathy, liver dysfunction, muscle weakness and mental retardation (Abdulhag et al., 2014).

Last respiratory complex in the electron transport chain, human mitochondrial complex V is the ATP synthase enzyme which produce ATP from ADP and inorganic phosphate(P_i) by using energy released from electrochemical gradient across the inner mitochondrial membrane (Jonckheere & Smeitink, 2012). Human mitochondrial complex V is formed from 14 subunits and two of them are encoded by mitochondrial DNA (Smeitink, Heuvel, & Dimauro, 2001).

1.4 Genetic Mapping of Disease Genes

Linkage analysis used for mapping disease genes is previously used technique to detect genes responsible for the development of Mendelian diseases and complex traits. Genetic mapping, also known as linkage mapping, gives indications that a parent-to-child transmitted disease is linked to one or more genes and gives insights into which chromosome contains the gene. Samples collected from family members with a certain disease or trait are used for the examination of unique patterns referred to as polymorphic markers that can only be seen in

family members with the disease or trait to detect which regions are shared by the affected individuals (Pulst, 1999).

In case of all family members with a specific disease or trait acquire a specific DNA marker, it is likely that the disease causing gene lies close to that marker. Because if a specific gene is close to the DNA marker, it is likely that the gene and marker will be inherited together. Linkage studies requires the use of large families that are phenotypically well characterized. Typically, smaller families can be used to track autosomal recessive disease while larger families can be used to track autosomal dominant diseases (Altshuler, Daly, & Lander, 2008).

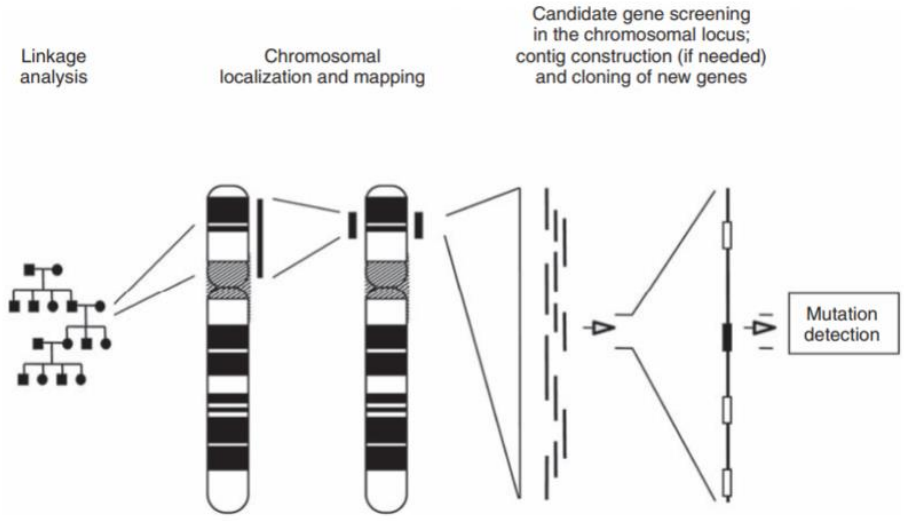

Figure 1.3 Identification of disease causing gene and variant by linkage mapping. Linkage maps are generated by using genetic markers to identify possible disease region on chromosome. Then, identified locus is screened for candidate gene (Menon, Trucco, Stratakis, & Sci, 2014)**.**

Since being first used for this purpose, types and the use of genetic markers have evolved significantly. One of the first available genetic markers was blood groups in the 1940s and it was followed by enzymes. Then, in 1980s and 1990s, development of restriction fragment length polymorphisms and short tandem repeats, respectively, made it possible to search for disease loci across genomes (Stein & Elston, 2009).

Huntington's disease which leads to progressive degeneration of brain's nerve cells and movement, cognitive and psychiatric dysfunctions was the first inherited disease mapped. In 1983, research indicated that the disease gene of Huntington's disease is associated with a polymorphic DNA marker mapping gene to human chromosome 4 (Gusella et al., 1983).

Today, rapid development of the Next Generation Sequencing (NGS) technology allows scientists to discover disease causing genes and variants within few days with high accuracy by integrating disease gene mapping and sequencing technology (Williams, 2018).

1.5 Next Generation Sequencing

After the development of first generation sequencing, chain termination method known as Sanger sequencing by Frederick Sanger and the chemical degradation method known as Maxam-Gilbert sequencing by Allan Maxam and Walter Gilbert in 1977, the need for highly automated, fast, cost-effective and accurate analyses of the genome paved the way for the development of next-generation sequencing (NGS) in the early 21st century (Barba, Czosnek, & Hadidi, 2014).

Next generation sequencing technologies, also known as high-throughput sequencing technologies or second generation sequencing, provide a massively parallel sequencing of multiple samples in one run with three basic steps: library preparation, amplification and sequencing.

Although having similar working principle with Sanger sequencing which relies on capillary electrophoresis and identification of nucleotides by emitted fluorescent signals in fragmented and amplified DNA, next generation sequencing provides higher throughput, higher sensitivity, faster and cheaper sequencing to get accurate information about the genome (Khalid & Ahmad, 2016).

Depending on the biological question, NGS technologies offer many different applications such as *de novo* sequencing to assemble novel genomes without reference sequence, DNA-sequencing (whole genome, whole exome and targeted sequencing), RNA-sequencing and epigenome sequencing to detect genetic variation , ChIP-seq (chromatin immunoprecipitation sequencing) to analyze DNA-protein interactions and CLIP-seq (cross-linking immunoprecipitation sequencing) to analyze RNA-protein interactions (Park, 2016).

Today, sequencing technologies are being developed continuously for different purposes in different fields. In addition to second generation sequencing, third generation technologies (also known as long-read sequencing) provides single molecule sequencing with longer reads (>10,000 bp) and highly accurate analysis of the genome (Lee et al., 2016).

1.5.1 Whole Exome Sequencing

Exons are nucleotide sequences that encode mature messenger RNA (mRNA) in RNA transcript and DNA sequence encoding it. The term exome refers to all exons of the genome. All exons make up 1% of the human genome and 85% of the known disease causing variants are represented by the exome. Due to its smaller size and higher contribution to development of diseases, exome sequencing and its analysis are crucial to understanding the genetics of human diseases (Choi et al., 2009).

So, as a cost effective alternative of whole genome sequencing (WGS), whole exome sequencing (WES) allows the detection of copy number variants (CNVs), structural variants (SVs), insertions and deletions (indels) and single nucleotide variants (SNVs) (Bao et al., 2014). WES is performed by using both *in silico* and wet-lab approaches. In wet-lab part, first step in WES is a construction of a library that includes DNA isolation and fragmentation into short segments. Adaptors are added to short DNA segments and exons are captured using biotinylated probes. Then, captured segments are amplified for the library enrichment and remaining DNA is separated from exomic DNA. After library enrichment, amplified exomic DNA segments are sequenced using different sequencing platforms (Keogh & Chinnery, 2013).

In silico part includes the analysis of raw data. First, short segment reads are mapped to reference genome and variant calling is performed. Then, annotation of variants is performed followed by filtration and prioritization of annotated variants (Foo, Liu, & Tan, 2012).

1.5.2 WES Analysis on RD-Connect Platform

Rare diseases (also known as orphan diseases) are diseases that affect a small number of the population. For example, in Europe, if the number of affected people is less than 5 per 10,000, a disease can be considered as a rare disease. In United States, a rare disease is defined as a condition affecting less than 200,000 people. So, there are different official definitions of a rare disease for each country.

Basic knowledge including the disease cause, pathophysiology, natural course and epidemiological data is limited or not available. This significantly hinders the diagnosis and treatment of rare diseases. Fundamental research in disease process is necessary both at the national and global level by establishing global networks (biobanks, registries, expertise networks etc.) to address this challenge (Weely et al., 2013).

RD-Connect is a platform that combines clinical and genomic data to enable researchers to discover disease causing genes, diagnostic options and potential therapies in the field of rare diseases.

Establishing patient registries and conformation of the diagnosis is very crucial in rare disease patients. RD-Connect platform provides Genome-Phenome Analysis Platform to analyze WGS and WES data by combining them with standardized phenotype data from PhenoTips platform. PhenoTips platform enables researchers and clinicians to collect phenotypic information including findings from physical examination, laboratory investigations, medical history of the patient and his/her family. Standardization of the patient registries in PhenoTips software is generated by using Human Phenotype Ontology (HPO) terms (Girdea et al., 2013).

To make data analysis easier, RD-Connect platform also developed new bioinformatics tools and integrated them to the Genome-Phenome Analysis Platform. Additionally, Sample Catalogue and Registry & Biobank Finder systems were developed by RD-Connect platform to allow researchers to access standardized information of other rare disease registries and their biosamples (Thompson et al., 2014).

1.5.3 Filters Used In WES Analysis

Mode of inheritance: variants can be prioritized according to mode of inheritance: inherited autosomal recessive, autosomal dominant and X-linked variants and de novo variants.

Coverage and read depth: the read depth indicates the number of reads at targeted genomic position (Sims, Sudbery, Ilott, Heger, & Ponting, 2014).

Alternative allele frequency: proportion of reads supporting the alternative allele rather than reference allele among all reads at specific position ("Variants, alleles and haplotypes | EMBL-EBI Train online," n.d.).

Impact prediction for a variant: it is important to predict variant impact to make filtering process easier by categorizing and prioritizing them. High, moderate, low and modifier terms are used to define the variant impact. Variant effect names are described by using Sequence Ontology (SO) terms. High impact indicates disruptive effect of a variant on protein structure such as protein truncation, loss of function or non-sense mediated decay. For example, stop-gained and frameshift variants. Moderate impact indicates non-disruptive effect of a variant on protein structure. It might change protein effectiveness. For example, missense variant and in-frame

deletion. Low impact indicates a variant that is mostly harmless and unlikely to change protein effectiveness. For example, synonymous variant, non-coding transcript variant or intronic variants in coding transcript. And lastly, modifier impact means hard-to-predict effects of a variant. For example, upstream and downstream gene variants, splicing variants (Cingolani et al., 2012)

Variant classification: variants can be classified into two groups: sequence variants and structural variants. Sequence variants are single nucleotide polymorphisms (SNPs) which refers to a change in a single DNA building block, insertions and deletions (indels) corresponding insertion or deletion of small segments of DNA and substitutions which means an exchange of single nucleotide or nucleotide sequence for another. Structural variants are copy number variations (CNVs), inversions and translocations. CNVs are changes in the copy number of a particular region. Inversion refers to an inversion of a segment of chromosome in the same region and translocation refers to a rearrangement of DNA segment between chromosomes (Hunt et al., 2018).

ClinVar classification: ClinVar is a free public archive hosted by the National Center for Biotechnology Information (NCBI). ClinVar database presents clinical significance of a certain variant by combining human variants and clinical phenotypes. ClinVar database receives submissions from clinical testing laboratories, research laboratories, professional organizations and groups. Database classifications can be “pathogenic” or “likely pathogenic” for variants considered as pathogenic, “benign” or “likely benign” for variants considered as benign and “uncertain significance” for variants with unknown significance (Gradishar, W., Johnson, K., Brown, K., Mundt, E., & Manley, 2017).

Population filters: Population filters include allele frequency in Exome Aggregation Consortium (ExAC) database, in 1000 Genome Project (1000GP) and Genome Aggregation Database (gnomAD) as well as internal allele frequency.

SNV effect prediction: Reliable prediction of deleteriousness of variants from NGS results is crucial for the detection of pathogenic variants. There are many different tools to estimate functional effect and score deleteriousness of variants i.e. PolyPhen-2, SIFT, MutationTaster, PROVEAN, FATHMM, PANTHER etc. (Dong et al., 2015). RD-Connect Platform uses MutationTaster, PolyPhen-2 and SIFT software tools to predict variant effect on protein structure.

"MutationTaster" assesses the pathogenic potential of alterations in DNA sequences. It is intended to predict the functional effects of amino acid substitutions, intronic and synonymous alterations, short indels, intron/exon border spanning variants. MutationTaster includes all known publicly available disease variants, SNPs and indels from integrated databases to analyze NGS results. MutationTaster uses Bayes classifier with different classification models for its predictions (Schwarz, Cooper, Schuelke, & Seelow, 2014).

"PolyPhen2" and "SIFT" are also tools that predicts the effects of amino acid substitutions using databases such as Protein Data Bank (PDB). Functional effect of the variant is predicted by using Bayes classifier (Adzhubei et al., 2010 ; (Sim et al., 2012)

CADD is a score used to rank deleteriousness of SNVs and short indels in coding and non-coding regions of the genome. CADD score integrates data from evolutionary, epigenetic, functional and genetic annotations. (Rentzsch, Witten, Cooper, Shendure, & Kircher, 2019)

1.6 Aim of the Study

Neurological diseases are among the most serious human challenges of the 21st century and it is important to understand how genetics can affect the initiation of neurological diseases and how clinical and pathological symptoms match genetic background.

The main aim of the project was to analyze molecular basis of hereditary neurological disorders in children by using whole exome sequencing, bioinformatics approaches and in vivo/in vitro functional studies. So, we planned to perform staged analysis of exome sequencing results for (1) assessment of the known genes, (2) discovery of the new causal genes and variants in neurogenetic diseases, (3) discovery of modifier genes that alter penetrance and expressivity of neurogenetic diseases and (4) comprehensive genome-wide analysis in unsolved families.

With whole exome sequencing in this large cohort, increasing the proportion of genetically diagnosed families, enabling reproductive counseling and disease-specific therapies, systematically deep phenotyping and explaining the genotype-phenotype relation in detail, improving biological understanding of rare childhood neurological disorders with functional in vivo and in vitro studies were also aimed.

To contribute to the Turkish genomic variome and generate a basis for future studies, it was aimed to create extensive data on a large cohort of Turkish consanguineous families that are available to authorized researchers around the world.

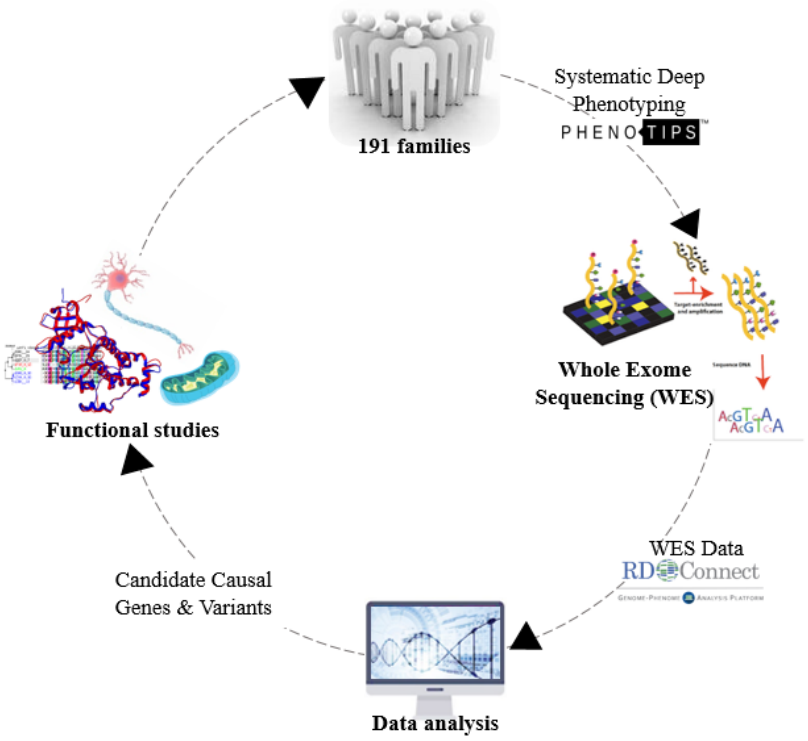

Figure 1.4 Experimental design of the study.

2. MATERIALS AND METHODS

2.1 Materials

2.1.1 Subjects in This Study

Three pediatric neurology clinics in Turkey: Izmir, Malatya and Diyarbakir recruited patients as part of the CONSEQUITUR project. Proband, affected/unaffected siblings and parents were enrolled in research protocol for diseases related to consanguineous marriages that was approved by Dokuz Eylul University, School of Medicine Institutional Review Board. Before participating the study, informed consent was obtained from both parents for whole exome sequencing and the publication of medical information. Disease groups analyzed in our study are given in **Figure 2.1**.

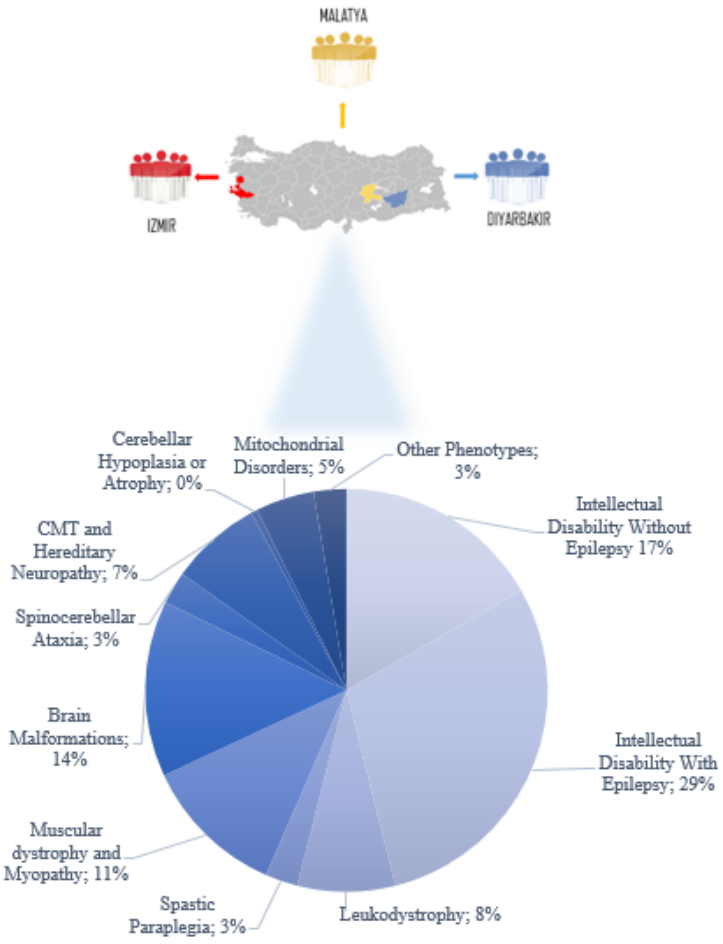

Figure 2.1 Disease groups analyzed in this study.

2.1.2 Buffers, Solutions and Other Materials Used in DNA Isolation

Buffers and solutions used in DNA isolation procedure are given in **Table 2.1**.

Table 2.1 Buffers and solutions used for DNA isolation.

Name	Components	Company / Cat No.	Description
5M Sodium perchlorate solution [$NaClO_4$ (H_2O)]	$NaClO_4$	Sigma-Aldrich / 310514	30.62 g of $NaClO_4$ was dissolved in enough water to make 50 mL of solution. Solution was stored at 4^0C.
0.5 M EDTA solution (pH 8.0)	EDTA NaOH	BioShop/ EDT001 Tekkim/ TK.170511.01002	46.5 g of EDTA was dissolved in 200 mL of dH_2O. pH was adjusted to 8.0 with ~5 g NaOH pellets. Volume was adjusted to 250 mL with H_2O. Solution was sterile filtered and stored at RT.
1 M Tris-HCl buffer (pH 8.0)	Tris HCl	BioShop/ TRS003 Merck / 100314	121.14 g of Tris were dissolved in enough water. pH was adjusted to 8.0 with HCl. Volume was adjusted to 1000 mL. Solution was autoclaved and stored at room temperature.
Tris-EDTA buffer	1 M Tris-HCl 0.5 M EDTA ; pH 8	- -	1 mL of 1 M Tris-HCl stock solution and 200 µL of 0.5 M EDTA (pH 8.0) were added to 98.8 mL of dH_2O to make 100 mL of solution. Solution was autoclaved and stored at room temperature.
10% SDS solution	SDS	Sigma-Aldrich/ L3771	10 g of SDS were dissolved in enough water to make 100 mL of solution. Solution was stored at room temperature.
40% NaOH buffer	NaOH	-	40 g of NaOH were dissolved in enough water to make 100 mL of solution. Solution was stored at room temperature.

Table 2.1 Buffers and solutions used for DNA isolation (Continued).

Name	Components	Company / Cat No.	Description
Buffer A	10 mM Tris-HCl 320 mM sucrose 5 mM $MgCl_2$ Triton X-100	Sigma-Aldrich / T5941-500G Merck/ 107651 Tekkim / TK.120290.01003 Thermo Scientific/ BP151-500	1.21 g of Tris-HCl, 109.55 g of sucrose and 1.02 g of $MgCl_2$ dissolved in 800 mL of dH_2O. pH was adjusted to 8.0 with 40% NaOH. Volume was adjusted to 990 mL and solution was autoclaved. Once autoclaved, 10 mL of triton X-100 was added. Solution was stored at 4^0C.
Buffer B	400 mM Tris-HCl 0.5 M EDTA; pH 8.0 150 mM NaCl 10% SDS	- - Tekkim / TK.170540-01000 -	30.50 g of Tris-HCl, 60mL of 0.5 M EDTA and 4.40 g of NaCl dissolved in 350 mL of dH_2O. pH was adjusted to 8.0 with 40% NaOH. Volume was adjusted to 450 mL and solution was autoclaved. Once autoclaved, 50 mL of 10% SDS was added and solution was mixed well by gently inverting. Solution was stored at room temperature.
1% Agarose gel	Agarose powder 1X TAE buffer SafeView™ DNA stain	BioShop/AGA003.500 BioShop / TAE222.1 Abm / G108	1 g of agarose powder was mixed with 100 mL of 1X TAE buffer and solution was microwaved for 1.5-2 min. 5 µL of SafeView™ DNA stain was added to agarose solution.

Table 2.2 Other materials used for DNA isolation and quantification.

Component	Company / Cat No.
6X loading dye	NEB / B7024S
Molecular weight ladder	NEB / N3231S

2.1.3 Buffers, Solutions and Other Materials Used In Blue Native Polyacrylamide Gel Electrophoresis (BN-PAGE)

Buffers and solutions used for BN-PAGE are given in **Table 2.3.**

Table 2.3 Buffers and solutions used for sample preparation and BN-PAGE.

Name	Components	Company / Cat No.	Description
3X Gel Buffer	1.5 M aminocaproic acid 150 mM Bis-Tris; pH 7.0 HCl	Sigma-Aldrich / A2504-100G Sigma-Aldrich / B9754-100G -	19.68 g aminocaproic acid, 3.14 g Bis-Tris were dissolved in dH_2O. pH was adjusted to 7.0 with HCl. Total volume was adjusted to 100mL. Solution was sterile filtered and stored at 4^0C.
Membrane Buffer	3X gel buffer 2 M aminocaproic acid 500 mM EDTA	- - -	0.5 mL 3X gel buffer, 0.5 mL 2 M aminocaproic acid and 4 µl 500 mM EDTA solution were sterile filtered and stored at 4^0C.
SBG Sample Buffer	0.75 M aminocaproic acid 5% Coomasie Brillant Blue G250	- Bio-Rad / 161-0406	3.75 mL of 2 M aminocaproic acid and 5 g Coomasie Brillant Blue G250 were dissolved in dH_2O. Solution was sterile filtered and stored at RT.
Cathode Buffer	15 mM Bis-tris 50 mM tricine HCl	- Sigma-Aldrich / T0377-100G -	3.14 g Bis-tris, 8.96 g tricine were dissolved in dH_2O. pH was adjusted to 7.0 with HCl. Total volume was adjusted to 1 L. Solution was stored at 4^0C.
Blue Cathode Buffer	Cathode buffer 0.02% Coomasie Brillant Blue G250	- -	0.02 g Coomasie Brillant Blue G250 was dissolved in 100 mL of cathode buffer. Solution was stored at 4^0C.

Table 2.3 Buffers and solutions used for sample preparation and BN-PAGE (Continued).

Name	Components	Company / Cat No.	Description
Anode Buffer	50 mM Bis-tris HCl	- -	20.93 g Bis-tris was dissolved in dH_2O. pH was adjusted to 7.0 with HCl. Total volume was adjusted to 2 L. Solution was stored at 4^0C.
Digitonin solution	Digitonin (4mg/mL)	Sigma-Aldrich / D141-100MG	0.004 g digitonin was dissolved in PBS with protease inhibitor in water bath at 37^0C.

Table 2.4 Other materials used for BN-PAGE.

Component	Company / Cat No.
Protein standard	Thermo Scientific / LC0725
NativePAGE™ Bis-Tris Protein Gels (3-12% & 4-16%)	Thermo Scientific / BN1001 & BN1002
Lauryl maltoside (10%)	Abcam / Ab109857
Protease inhibitor cocktail	Roche / 05892791001

2.1.4 Buffers, Solutions and Other Materials Used In Sodium Dodecyl Sulfate Polyacrylamide Gel Electrophoresis (SDS-PAGE) and Western Blotting.

Buffers and solutions used in Sodium Dodecyl Sulfate Polyacrylamide Gel Electrophoresis (SDS-PAGE) and western blotting are given in **Table 2.5**.

Table 2.5 Buffers and solutions used for SDS-PAGE and western blotting.

Name	Components	Company / Cat No.	Description
Blocking solution	Bovine serum albumin (BSA) Non-fat dry milk powder 1X TBST	Sigma-Aldrich / A2058 Cell Signaling / 9999S -	1 g of BSA or Non-fat dry milk powder were dissolved in 20 mL of 1X TBST. Fresh solution was prepared for each use.
10X running buffer	25 mM Tris 192 mM Glycine 0.1% SDS	- Sigma-Aldrich / G8898-500G -	15 g Tris base and 71.2 g Glycine were dissolved in dH_2O. 50 mL 10% SDS was added and total volume was adjusted to 1 L.
10X transfer buffer	20 mM Tris Base 150 mM Glycine 0.0375 %SDS	- - -	24.2 g Tris base and 112.5 g glycine were dissolved in dH_2O. 37.5 mL 10% SDS was added to solution. Total volume was adjusted to 1 L. Solution was stored at 4^0C.
1X transfer buffer	10X transfer buffer Methanol	- Merck / 106009	100 mL of 10X transfer buffer and 200 mL of methanol were added to 700 mL of dH_2O. Fresh buffer was prepared for each use.
10X TBS	Tris-HCl NaCl	- -	24.23 g Tris-HCl and 80.06 g NaCl were dissolved in water. Total volume was adjusted to 1 L.
1X TBST	10X TBS Tween-20	- Sigma-Aldrich / P1379-1L	100 mL 10X TBS and 1 mL Tween-20 were added to dH_2O. Total volume was adjusted to 1 L.

Table 2.5 Buffers and solutions used for SDS-PAGE and western blotting (Continued).

Name	Components	Company / Cat No.	Description
5% SDS-Polyacrylamide stacking gel	Acrylamide bisacrylamide (30%)	Sigma-Aldrich / A3574-100ML	1.6 mL acrylamide bisacrylamide solution, 2.5 mL Tris-HCl, 100 µL 10% SDS, 10 µL TEMED and 100 µL APS were added to 5.7 mL dH_2O.
	0,5 M Tris-HCl	-	
	10%SDS	-	
	TEMED	Sigma-Aldrich / T7024-100ML	
	APS (10%)	Sigma-Aldrich / A3678-100G	
10% SDS-Polyacrylamide separating gel	Acrylamide bisacrylamide (30%)	-	3.3 mL acrylamide bisacrylamide solution, 2.5 mL Tris-HCl, 100 µL 10% SDS, 10 µL TEMED and 100 µL APS were added to 4 mL dH_2O.
	1,5 M Tris-HCl	-	
	10%SDS	-	
	TEMED	-	
	APS (10%)	-	

Table 2.6 Other materials used for SDS-PAGE and western blotting.

Component	Company / Cat No.
Color pre-stained protein standard	NEB / P7712
Western HRP substrate	Merck / WBLUF0500
Sample loading buffer	Cell Signaling / 7722S

2.1.5 Media and Solutions Used In Cell Culture

Components used in preparation of cell culture media and other materials are given in **Table 2.7** and **Table 2.8**, respectively.

Table 2.7 Materials used for preparation of cell culture media.

Name	Components	Company / Cat No.	Description
10% and 30% FBS Fibroblast Media	DMEM (Dulbecco's Modified Eagle Medium)	Gibco / 41966029	DMEM media with 10% or 30% FBS, 1X Penicillin-Streptomycin, 2.5 ug/ml Amphotericin B was prepared and stored at 4^0C.
	Penicillin-Streptomycin 100X	Gibco / 15140122	
	Amphotericin B	Gibco / 15290018	
	FBS (Fetal Bovine Serum)	Gibco / 10500064	

Table 2.8 Other solutions, media and used in cell culture.

Component	Company / Cat No.
1X PBS (Phosphate-Buffered Saline)	Gibco / 10010023
Trypsin-EDTA (0.25%)	Gibco / 25200072
RPMI 1640 Medium, no phenol red	Gibco / 11835030
MitoTracker® Red CMXRos	Thermo Scientific / M7512
Hoechst 33342	Thermo Scientific / 62249

2.1.6 Commercial Kits

Commercial kits used in this study are given in **Table 2.9**.

Table 2.9 Commercial kits used in the study.

Component	Company / Cat No.
NucleoSpin® RNA Isolation Kit	MACHEREY-NAGEL / 740955.50
Pierce™ Coomassie Plus (Bradford) Assay Kit	Thermo Scientific™ / 23236
NucleoSpin® Blood L Kit	MACHEREY-NAGEL / 740954.20
ProtoScript® First Strand cDNA Synthesis Kit	NEB / E6300S
NucleoSpin® TriPrep Kit	MACHEREY-NAGEL / 740966.50
Q5® High-Fidelity DNA Polymerase Kit	NEB / M0491S

2.1.7 Primers

Primers and their sequences used in Sanger verification and cDNA sequencing are given in **Table 2.10**. Oligos were purchased from Oligomer Biotechnology, Turkey.

Table 2.10 Primers and sequences used in this study.

Primer	Sequence (5'→ 3')	Tm	GC%	Product
PTPMT1 Sanger Fw	GTCTCCACCGTCTTTGCTGA	59^0C	55%	206 bp
PTPMT1 Sanger Rv	CACACTTCTCTAGCCGTCCC	59^0C	60%	
PTPMT1 cDNA Fw	CTGCTCTACACCCTGTTCCG	61^0C	60%	520 bp
PTPMT1 cDNA Rv	TGTTGCCCGTGCAGTAATCT	57^0C	50%	

2.1.8 Antibodies

Antibodies used in this study are given in **Table 2.11**.

Table 2.11 Antibodies used in this study.

Antibody	Company / Cat No.
Total OXPHOS Blue Native WB Antibody Cocktail	Abcam / ab110412
PTPMT1 Antibody (B-3)	Santa Cruz Biotechnology / sc-390901
Anti-beta Actin antibody	Abcam / ab8227

2.1.9 Equipment

The equipment used in this study are listed in **Table 2.12.**

Table 2.12 The equipment used in the study.

Equipment	Company
Laminar air flow cabinet	Thermo Scientific
Pipettes	Biohit, Thermo Scientific
Serological pipette	Isolab, Sarstedt
Pipette tips	Biosphere, Tarsons
Centrifuges	Thermo Scientific
Microwave	Beko
Gloves	Isolab
Parafilm	Isolab
Eppendorf-falcon tubes	Sarstedt, Corning
Cell culture incubator	Eppendorf, Thermo Scientific
Nitrogen tank	Taylor – Wharton
Tissue culture flask (T25, T75)	Sarstedt
Culture plates	Sarstedt
Glass bottom confocal plate	Corning
Petri dishes	Sarstedt, Isolab
PVDF membrane	Bio-Rad
Vortex	Thermo Scientific
Balance	Sartorius
Quick spin	Thermo Scientific
Magnetic stirrer	Daihan Scientific
pH meter	Hanna

Table 2.12 The equipment used in the study (Continued)

Equipment	Company
Thermal cycler	Life Technologies
Horizontal gel electrophoresis system	Bio-Rad
Vertical gel electrophoresis system	Bio-Rad
Power supply	Bio-Rad
Electrophoretic Transfer Cell	Bio-Rad
Light microscope	Zeiss
Thoma counting chamber	Isolab
Ice machine	Hoshizaki
Spectrophotometer	Bio-Rad
Water Bath	Nüve

2.2 Methods

2.2.1 DNA Isolation from Peripheral Blood Sample

Protocol of DNA isolation using sodium perchlorate was adapted from Johns & Paulus-Thomas, 1989. Peripheral blood stored in EDTA containing tubes was collected from all participants. DNA isolation from 1 mL of peripheral blood sample was done according to standard protocol.

Before initiating the isolation, aliquots of chloroform were chilled at -20^{0}C and water bath was set to 65^{0}C. In the cell preparation step, 1 mL of peripheral blood was thawed in the hand and poured into a 50 mL sterile centrifuge tube as soon as possible. Then, 20 mL of Buffer A was added to centrifuge tube and shaken for 4 minutes at room temperature. After shaking, tube was centrifuged for 10 minutes at 3,000 rpm. Supernatant was discarded and pellet was resuspended in 10 mL of Buffer A. Again, suspension was shaken for 4 minutes at room temperature and centrifuged for 10 minutes at 3,000 rpm. After centrifuge, supernatant was discarded.

In the cell lysis step, cell pellet from previous step was resuspended in 1 mL of Buffer B by vortexing. Suspension was transferred into a 15 mL centrifuge tube. 500 µl of sodium perchlorate was added and suspension was shaken for 10 minutes at room temperature. After shaking, suspension was incubated for 25 minutes at 65^{0}C by quickly vortexing every 5 minutes.

In DNA extraction step, centrifuge was set to 4^0C firstly. 2 mL of chloroform (-20^0C) was added to suspension from previous step and suspension was shaken for 10 minutes at room temperature. Then it was centrifuged for 10 minutes at 3,000 rpm. In the meantime, 15 mL centrifuge tube with 3 ml of ethanol (98%) and 1.5 mL Eppendorf tube with 500 µl of ethanol (70%) was prepared. After centrifuge, supernatant was transferred into a 15 mL centrifuge tube containing 3 ml of ethanol (98%) and mixed gently by inverting ~20 times until the DNA precipitate "Medusa" is visible. Then, "Medusa" was captured by using micropipette and transferred into a 1.5 mL Eppendorf tube containing 500 µl of ethanol (70%). Tube was spinned down for 1 minute at 14,000 rpm using Eppendorf microcentrifuge. Ethanol was removed and pellet was allowed to dry for ~25 minutes at room temperature. Then, pellet was dissolved in 50 µl of Tris-EDTA buffer and incubated overnight at 4^0C.

After 24 hours, sample was heated at 54^0C to make sure DNA has fully dissolved and DNA concentration was measured using NanoDrop spectrophotometer. Quality of the isolated DNA was checked by running the sample on a 1% agarose gel.

2.2.2 Whole Exome Sequencing and Data Analysis

Whole exome sequencing (WES) was performed at the Broad Institute of MIT and Harvard, using Illumina Exome Capture Kit (38 Mb target). Sequencing data was processed at the Centro Nacional de Análisis Genómico (CNAG), Barcelona by using Picard based pipeline and data analysis was carried out on the RD-Connect Genome-Phenome Analysis Platform (https://platform.rd-connect.eu/genomics) using standard filtering criteria for rare diseases, including Minor Allele Frequency (MAF)< 1%, Variant Effect Predictor (VEP)=moderate/high and Combined Annotation Dependent Depletion (CADD) >20.

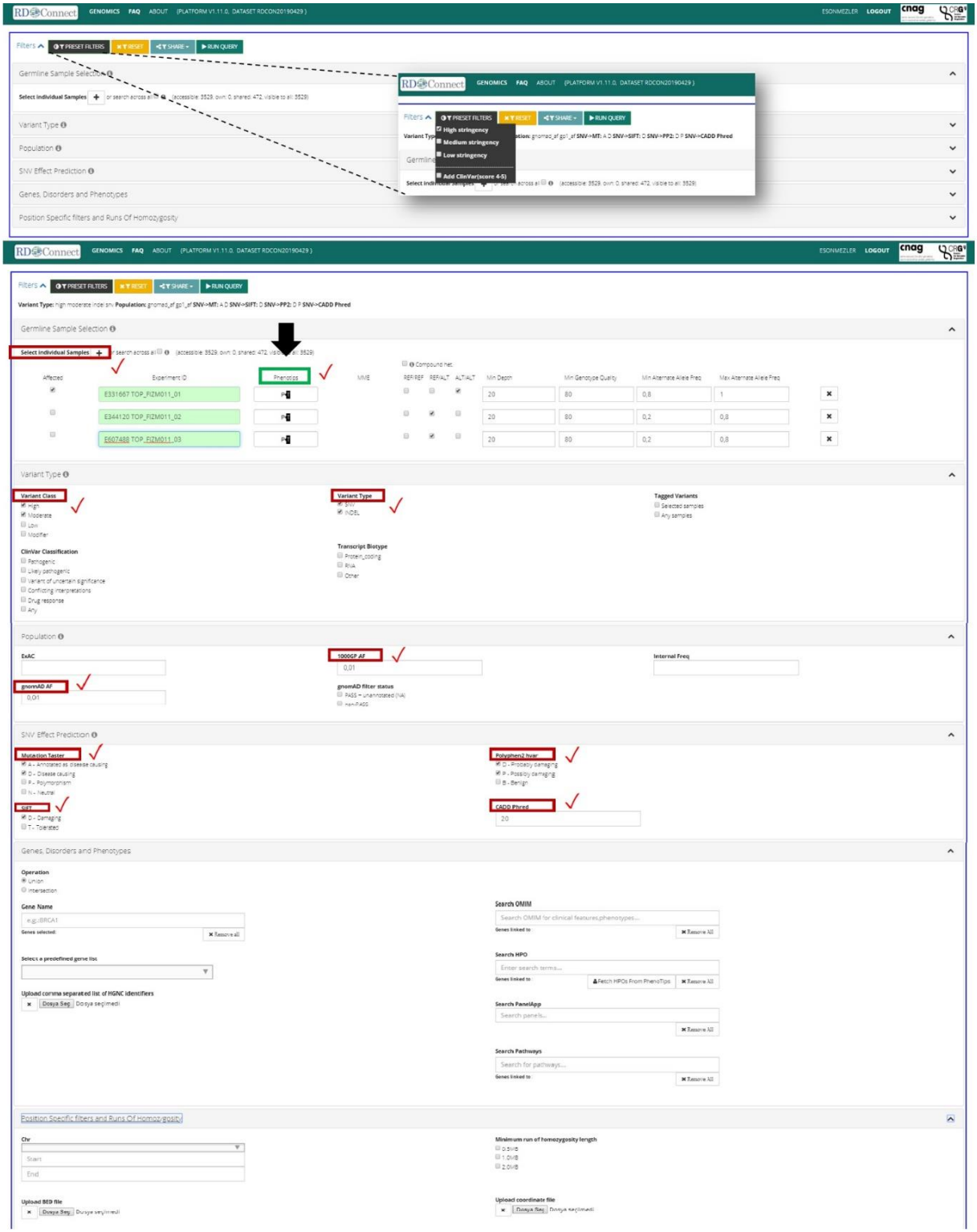

Figure 2.2 WES data analysis and filtering process on RD-Connect platform. MAF< 1%, VEP=moderate/high and CADD >20 were used for standard filtering criteria for rare diseases.

2.2.3 Derivation and Maintenance of Patient Fibroblasts

Patient fibroblasts used in our study were obtained from a skin punch biopsy. Skin biopsy was taken by using a sterile 3 mm punch biopsy apparatus after disinfecting and anesthetizing the skin part. Biopsy was rinsed twice with DPBS and epidermis and subcutaneous fat part was removed by using sterile scalpel. Dermis part was dissected into 4-5 evenly sized pieces and each tissue piece was placed into each well of the 6-well plate containing 1 µl of FBS. Then, plate was incubated at 37^0C, 5% CO_2 for 30 minutes to better attachment of dermis pieces. After 30 minutes, 1 mL of DMEM media including 30% FBS, 1% penicillin-streptomycin-amphotericin B was added to the each well of 6-well plate. After 2 days, amount of media was increased to 2 mL. Media change was done every 2-3 days.

After approximately two weeks, when fibroblasts reached confluency around the tissue parts, fibroblasts in each well were washed once with DPBS and trypsinized with 1 mL of 0.25% trypsin/EDTA. After incubating plate at 37^0C, 5% CO_2 for 4 minutes, 2 mL of DMEM media including 30% FBS, 1% penicillin-streptomycin-amphotericin B was added to neutralize the 0.25% trypsin/EDTA. Collected fibroblasts were transferred to 15 mL centrifuge tube and centrifuged at 1400 rpm for 2 minutes. After centrifuge, supernatant was discarded and cell pellet was resuspended in 4 mL of DMEM media including 30% FBS, 1% penicillin-streptomycin-amphotericin B. Suspension was transferred to T25 flask and cells were expanded by changing the media every 2-3 days. After reaching confluency, cells were transferred to T75 flask. Fibroblasts around the tissue parts can be collected up to 3^{rd} passage. When fibroblasts were expanded, they were frozen down using freezing media containing 10% DMSO and 90% FBS and stored in liquid nitrogen for long-term storage.

2.2.4 Blue Native Polyacrylamide Gel Electrophoresis (BN-PAGE) For Mitochondrial Complex Analysis

BN-PAGE is a powerful method used for the isolation of intact multiprotein complexes. Native separation of protein complexes on polyacrylamide gel relies on the Coomasie blue dye which gives negative charge to the protein complexes without denaturing them. To analyze individual subunits of the protein complexes, second dimension SDS-PAGE can be applied under denaturing conditions.

Sample preparation from patient fibroblasts for BN-PAGE: cells from fully confluent T75 flask were detached by adding 1 mL of 0.25% trypsin/EDTA. 2 mL of DMEM media including 10% FBS, 1% penicillin-streptomycin was added to neutralize the 0.25% trypsin/EDTA. Then, suspension was transferred to 15 mL centrifuge tube and centrifuged at 1200 rpm for 2 minutes at 4^0C. Cell pellet was washed with chilled PBS and centrifuged again at 1200 rpm for 2 minutes at 4^0C. After second centrifuge, cell pellet was resuspended in 500 µL ice cold protease inhibitor dissolved in PBS. To measure protein concentration, 10 µL of cell suspension was lysed with 0.1% Triton X-100 in PBS and protein concentration was measured using Bradford Assay. Then, cells were resuspended in PBS with protease inhibitor to a final concentration of 5 mg/mL by adjusting total volume to 400 µL. Fibroblasts were lysed by adding equal volume (400 µL) of 4 mg/mL digitonin solution to make digitonin/protein ratio 0.8 and permeabilize cellular and nuclear membranes. Solution was vortexed and incubated on ice for 5 minutes. Then, solution was centrifuged at 10 000 rcf for 10 minutes to extract mitochondria. Supernatant was removed and pellet was resuspended in membrane buffer. 10% dodecyl maltoside was added to a final concentration of 1% (1/10 volume of membrane buffer added) to stabilize and activate enzymes for membrane researches. After vortexing the solution, it was incubated on ice for 15 minutes and centrifuged at 20 000 rcf for 20 minutes at 4^0C. Supernatant was transferred to a new chilled microfuge tube and protein concentration was measured using Bradford Assay. SBG sample buffer (half of the volume of 10% dodecyl malthoside added in previous step) was added to 15-30 µg of sample. Final volume of the sample was adjusted to 20 µL by adding water. Remaining sample was stored frozen at -80^0C.

Blue Native gel electrophoresis: comb was removed from precast gel and the wells were rinsed with 1X NativePAGE™ Dark Blue Cathode Buffer three times. White tape near the bottom of the gel cassette was removed and gel was placed in the running tank. Samples were loaded into wells of Invitrogen NativePAGE Bis-Tris Precast Gel with Thermofisher NativeMark™ Unstained Protein Standard loaded into first lane. After loading samples and protein standard, upper cathode buffer chamber was filled with 1X NativePAGE™ Dark Blue Cathode Buffer and lower anode buffer chamber was filled with 1X NativePAGE™ Anode Buffer. Blue Native gel was run for 120-150 minutes at 100 V constant. After approximately 40 minutes, when the dye front has migrated about 1/3 of the way down the gel, 1X NativePAGE™ Dark Blue Cathode Buffer was replaced with 1X NativePAGE™ Light Blue Cathode Buffer to remove excess Coomassie blue dye.

Immunoblotting of Blue Native gel: after running the gel, protein complexes on the Blue Native gel were transferred to PVDF membrane. First, PVDF membrane was incubated in methanol for 1 minute and rinsed with distilled water three times. Dark blue dye accumulated at the bottom of the gel was removed with the help of the scalpel to prevent Coomassie dye interfering with the antibody binding. Transfer sandwich was prepared by placing PVDF membrane and Blue Native gel together with filter papers and placed into the tank. Tank was filled with SDS containing transfer buffer and protein complexes were transferred at 250 mA for 2 hours. Following transfer, PVDF membrane was rinsed quickly in methanol to remove excess Coomassie dye present. After rinsing the methanol with distilled water, membrane was blocked in 5% milk powder in TTBS for 1 hour at room temperature with gentle agitation. Then, membrane was incubated with Total OXPHOS Blue Native WB Antibody Cocktail diluted 1:250 in 5mL of blocking buffer overnight at 4^0C with gentle agitation. Following primary antibody incubation, membrane was washed 3x10 minutes in TTBS. Then, membrane was incubated with secondary antibody Rabbit Anti-Mouse Ig-HRP diluted 1:2000 in 14 mL of blocking buffer for 1 hour at room temperature. Following secondary antibody incubation, membrane was washed 4x5 minutes in TTBS. For the chemiluminescent detection of protein complexes, excess TTBS was removed from membrane and membrane was incubated with ECL substrate solution mix. After incubation, excess ECL substrate solution was removed and protein bands were visualized and analyzed with *ChemiCapt* software. Membrane was stored at 4^0C with enough TTBS.

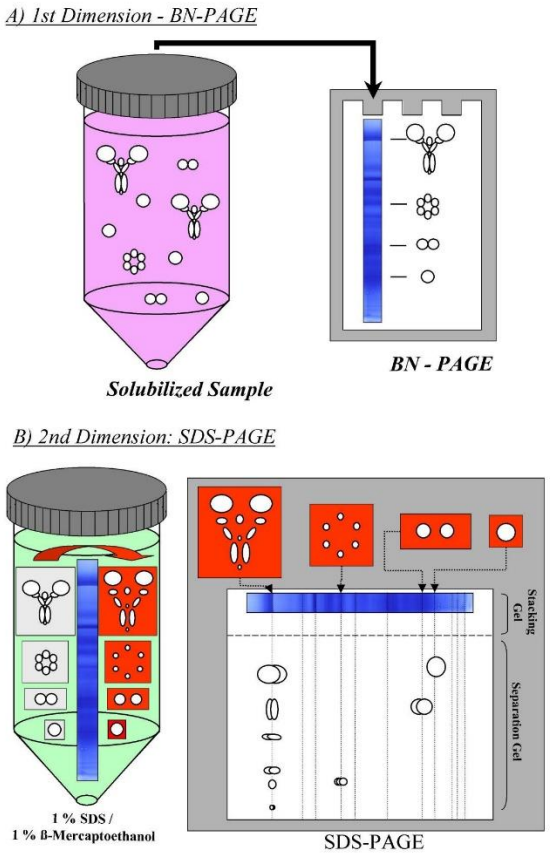

Figure 2.3 1st dimension BN-PAGE and 2nd dimension SDS-PAGE. (a) Separation of native protein complexes according to their molecular weight occurs at 1st dimension BN-PAGE under non-denaturant conditions. **(b)** Separation of subunits of protein complexes under denaturant conditions occurs at 2nd dimension SDS-PAGE (Eubel, Braun, & Millar, 2005).

2.2.5 RNA Isolation from Patient Fibroblasts

RNA was isolated from patient fibroblasts using the NucleoSpin® RNA Isolation Kit (MACHEREY-NAGEL). First, up to 5 x 10^6 cultured fibroblasts were collected by centrifugation. Cell pellet was lysed by addition of 350 µL lysis buffer RA1 and 3.5 µL β-mercaptoethanol and vortexing. To reduce viscosity and clear lysate, mixture was passed through a 0.9 mm needle firstly. Then, NucleoSpin® Filter (violet ring) was placed in a 2 mL collection tube, lysate was applied and centrifuged at 11,000 x g for 1 minute. NucleoSpin® Filter was discarded and 350 µL 70% ethanol was added to homogenized lysate. Lysate was mixed well by pipetting to adjust RNA binding to the column. Then, NucleoSpin® RNA Column (light blue ring) was placed in a 2 mL collection tube and lysate from previous step was loaded to the column after pipetting up and down 2-3 times. Lysate was centrifuged at 11,000 x g for 30 seconds and column was placed to a new 2 mL collection tube. Following

RNA binding step, 350 µL membrane desalting buffer MDB was added to the column and tube was centrifuged at 11,000 x g for 1 minute to dry the membrane. Then, DNase reaction mixture was prepared by mixing 10 µL reconstituted rDNase (according to section 3 "Storage conditions and preparation of working solutions) and 90 µL of Reaction Buffer for rDNase. 95 µL DNase reaction mixture was applied to the center of the silica membrane and incubated at room temperature for 15 minutes. Following RNA digestion, 200 µL wash buffer RAW2 was added to the NucleoSpin® RNA Column and centrifuged at 11,000 x g for 30 seconds. Column was placed to the new 2 mL collection tube. For the second wash, 600 µL wash buffer RA3 was added to the NucleoSpin® RNA Column and centrifuged at 11,000 x g for 30 seconds. Flow-through was discarded and column was placed back into the 2 mL collection tube. For the third wash, 250 µL wash buffer RA3 was added to the NucleoSpin® RNA Column and centrifuged at 11,000 x g for 2 minutes to dry the membrane completely. Then, column was placed into a supplied 1.5 mL nuclease-free collection tube. Following wash steps, RNA was eluted by adding 50 µL RNase-free H_2O to the column and centrifuging at 11,000 x g for 1 minute. RNA concentration and quality was checked using NanoDrop spectrophotometer. Sample was stored frozen at -80^{0}C.

2.2.6 cDNA Synthesis from RNA

cDNA synthesis from RNA samples was performed by using ProtoScript® First Strand cDNA Synthesis Kit (NEB). 1-6 µL RNA sample, 2 µL random primer mix (combination of $d(T)_{23}VN$ and hexamer primers) and variable amount of nuclease-free H_2O were mixed in a sterile RNase-free microfuge tube to make total volume 8 µL. RNA was denatured for 5 minutes at 70^{0}C to increase cDNA yield. Then, tube was spinned briefly and put promptly on ice. Following denaturation, 10 µL M-MuLV Reaction Mix (combination of dNTPs and optimized buffer) and 2 µL M-MuLV Enzyme Mix (combination of M-MuLV Reverse Transcriptase and murine RNase inhibitor) were mixed and added to 8 µL mixture from previous step. Total 20 µL reaction mixture was incubated at 25^{0}C for 5 minutes firstly and then, 42^{0}C for 1 hour. At the last step, enzyme was inactivated by incubating reaction mixture at 80^{0}C for 5 minutes. The cDNA product was stored at -20^{0}C.

2.2.7 Protein Isolation from Patient Fibroblasts

Total protein was isolated from patient fibroblasts using the NucleoSpin® TriPrep Kit (MACHEREY-NAGEL). First, up to 5 x 10^6 cultured fibroblasts were collected by centrifugation. Cell pellet was lysed by addition of 350 µL lysis buffer RA1 and 3.5 µL β-mercaptoethanol and vortexing. To reduce viscosity and clear lysate, mixture was passed through a 0.9 mm needle firstly. Then, lysate was filtrated through NucleoSpin® Filter (violet ring). NucleoSpin® Filter was placed in a 2 mL collection tube, mixture was applied and centrifuged at 11,000 x g for 1 minute. NucleoSpin® Filter was discarded and 350 µL 70% ethanol was added to homogenized lysate. Lysate was mixed well by pipetting to adjust RNA binding to the column. Then, NucleoSpin® RNA Column (light blue ring) was placed in a 2 mL collection tube and lysate from previous step was loaded to the column after pipetting up and down 2-3 times. Lysate was centrifuged at 11,000 x g for 30 seconds. To isolate protein, flow-through was recovered and transferred into a new 1.5 mL collection tube provided. One volume of protein precipitator PP was added and mixture was mixed vigorously. Then, mixture was incubated at room temperature for 10 minutes and centrifuged at 11,000 x g for 5 minutes. After centrifuge, supernatant was removed as completely as possible and 500 µL 50% ethanol was added to the pellet. Mixture was centrifuged at 11,000 x g for 1 minute and supernatant was removed again. Protein pellet was dried at room temperature for 5-10 minutes by keeping lid open. To prepare protein sample, 50 µL protein solving buffer-reducing agent mixture PSB-TCEP was added to dissolve protein pellet and mixture was incubated at 95-98^{0}C for 3 minutes to completely denature protein sample. Following incubation, sample was let cool down to room temperature and centrifuged at 11,000 x g for 1 minute to remove insolvable materials from the sample. Protein sample was stored at -20^{0}C.

2.2.8 SDS-PAGE (sodium dodecyl sulphate-polyacrylamide gel electrophoresis) And Western Blotting

SDS-PAGE is a widely used laboratory technique to separate proteins based on their molecular weight. 5% stacking gel and 10% separating gel were used to separate protein samples. First, 5 mL of separating gel mixture was poured between glass plates and 50% isopropanol was added immediately onto separating gel part to flatten the gel surface. First part of the gel was left for polymerization at room temperature for 15-20 minutes. Then, isopropanol

was removed completely from the polymerized gel and 2 mL stacking gel mixture was added onto polymerized sepating gel part. Comb was placed and gel was left for polymerization at room temperature for 15-20 minutes again. Following polymerization, comb was removed and gel was placed into the running tank. Tank was filled with running buffer and prepared protein samples from previous steps were loaded into the wells. Samples were run at 15 mA for 30 minutes and then, 18-20 mA for one hour.

After SDS-PAGE, protein samples on the gel were transferred to PVDF membrane. First, PVDF membrane was incubated in methanol for 1 minute and rinsed with distilled water three times. Transfer sandwich was prepared by placing PVDF membrane and gel together with filter papers and placed into the tank. Tank was filled with transfer buffer and proteins were transferred at 250 mA for 2 hours at 4^0C. Following transfer, proteins on the PVDF membrane were stained with Ponceau S. After confirming the presence of proteins, Ponceau S solution was rinsed with distilled water and membrane was blocked with blocking solution (5% BSA in TTBS) for 1 hour at room temperature with gentle agitation. Then, membrane was incubated with primary antibody (1:1000 diluted in blocking solution) for 1 hour at room temperature or overnight at 4^0C with gentle agitation. Following primary antibody incubation, membrane was washed 3x10 minutes in TTBS. Then, membrane was incubated with secondary antibody (1:2000 diluted in blocking solution) for 1 hour at room temperature. Following secondary antibody incubation, membrane was washed 3x10 minutes in TTBS. β-actin was used as internal control for the western blotting experiments. For the chemiluminescent detection of proteins, excess TTBS was removed from membrane and membrane was incubated with ECL substrate solution mix. After incubation, excess ECL substrate solution was removed and protein bands were visualized and analyzed with *ChemiCapt* software. Membrane was stored at 4^0C with enough TTBS.

2.2.9 Conventional Polymerase Chain Reaction (PCR) and Agarose Gel Electrophoresis

Potential causal variants from WES data analysis and their segregation were validated by PCR following Sanger sequencing. Primers spanning the region containing causal variant were designed by using NCBI Primer Designing Tool (https://www.ncbi.nlm.nih.gov/tools/primer-blast/). Oligos were purchased from Oligomer Biotechnology, Turkey. 100 μM stock solutions and 10 μM working solutions were prepared by dissolving lyophilized primers in Tris buffer, pH 8.0.

Polymerase Chain Reaction is a commonly used laboratory technique relies on thermal cycling to amplify specific segment of DNA molecule. *Q5*® High-Fidelity DNA Polymerase Kit (NEB) was used to set up reactions. Required reagents and conditions for PCR are shown below in **Table 2.13** and **Table 2.14**, respectively.

Table 2.13 PCR reagents.

Component	Volume
5X Q5 Reaction Buffer	5 µL
10 mM dNTPs	0.5 µL
10 µM Forward Primer	1.25 µL
10 µM Reverse Primer	1.25 µL
Template DNA	Variable
Q5 High-Fidelity DNA Polymerase	0.25 µL
5X Q5 High GC Enhancer (optional)	5 µL
Nuclease-Free Water	to 25 µL

Table 2.14 PCR conditions

Step	Temperature	Time
Initial denaturation	98^0C	30 seconds
25-35 cycles	98^0C $50\text{-}72^0$C 72^0C	5-10 seconds 10-30 seconds 20-30 seconds/kb
Final extention	72^0C	2 minutes
Hold	4^0C	∞

1% agarose solution was poured into gel tray after placing well comb and let sit at room temperature for 20 minutes. Once solidified, agarose gel was placed into the gel tank and tank was filled with 1X TAE buffer until the agarose gel is covered. Molecular weight marker was loaded into the first lane of the agarose gel. Then, 5 µL of DNA samples were mixed with 1 µL of 6X loading dye and loaded into wells. Agarose gel was run at 90-100 V for about 1 hours.

2.2.10 Suggested Genetic, Laboratory and Clinical Prescreening

Prior to WES, some genetic, laboratory and clinical prescreening tests were performed for each disease group. Suggested genetic, laboratory and clinical prescreening tests were given in **Table 2.15**.

Table 2.15 List of suggested genetic, laboratory and clinical prescreenings.

Disease Group	Genetic prescreening	Laboratory prescreening	Clinical prescreening
Intellectual disability with epilepsy	Karyotype; CGH array; SCN1A; Angelman; CLP1 founder (Turkey)	Acylcarnitines, VLCFA, AFP, Urinary organic acid, amino acids	Brain MRI, EEG
Intellectual disability w/o epilepsy	Karyotype; CGH array; FRAXA (fragile X); CLP1 founder (Turkey)	Acylcarnitines, VLCFA, AFP, Urinary organic acid, amino acids	Brain MRI
Cortical and other structural brain malformations	Karyotype	CK	Brain MRI, EEG
Leukodystrophies	Direct gene testing if biochemical test reveals specific enzyme deficiency	VLCFA; phytanic acid, pristanic acid; lysosomal enzymes (white blood cells), hexosaminidase (white blood cells)	Brain MRI, EMG; Nerve Conduction Velocities
Spinocerebellar ataxias	Friedreich ataxia; CWF19L1 founder (Turkish)	Acylcarnitines, VLCFA, AFP, Urinary organic acid, amino acids, serum immuno electrophoresis	Brain MRI, Nerve conduction velocities, EMG, ophthalmology
Spastic paraplegia	SPG4, SPG7	Acylcarnitines, VLCFA, AFP, Urinary organic acid, amino acids, serum immuno electrophoresis	Brain MRI, spine MRI, nerve conduction velocities, EMG, ophthalmology

Table 2.15 List of suggested genetic, laboratory and clinical prescreenings (continued).

Disease Group	Genetic prescreening	Laboratory prescreening	Clinical prescreening
CMT and hereditary neuropathies	PMP22 del/dup; SMN1 deletion; NTRK1 Turkish founder; HMSN Lom/Russe/CMT4C gypsy founder; CLP1 founder (Turkey)	Acylcarnitines, VLCFA, AFP, Urinary organic acid, amino acids	Nerve conduction velocities, EMG, Repetitive stimulation
Muscular dystrophies and myopathies	Dystrophin MLPA; Myotonic Dystrophy type 1; ETFDH founder mutation (Turkey); SMN1 deletion; FSHD type 1; POMT1 founder (Turkey); PLEC founder (Turkey)	CK, Pompe dried blood spot	Muscle biopsy (histology), Muscle biopsy (immunohistochemistry, immunoblotting), Brain MRI, Nerve conduction velocities, EMG, Repetitive stimulation, echocardiography, electrocardiography
Congenital myasthenic syndromes	CHRNE sequencing; CHAT founder (Turkey)	CK	Nerve conduction velocities, EMG, Repetitive stimulation, Muscle biopsy
Mitochondrial disorders	MELAS mtDNA mutation, MERRF mtDNA mutation, NARP/MILS mtDNA mutation, ETFDH founder (Turkey), mtDNA single deletion (in blood)	Lactate, ALT/AST/GGT, glucose, blood cell count, CK	Muscle biopsy (COX, SDH), Brain MRI, Nerve conduction velocities, EMG, ophthalmology, echocardiography, electrocardiography, EEG, audiology
Cerebellar hypoplasia or atrophy	CLP1 founder (Turkey); CGH array (if combined with ID)		Brain MRI, Nerve conduction velocities, EMG, ophthalmology

2.2.11 Mitochondrial Staining in Patient Fibroblasts

24 hours before the experiment, 15 x 10^4 control and patient fibroblasts were plated in 35 mm glass bottom confocal dishes. At the day of experiment, growth media was removed from culture dishes and RPMI media with 100 nM MitoTracker® Red CMXRos and 1 μg Hoechst 33342 was added to fibroblasts. Culture plates were incubated at 37^0C, 5% CO_2 for 15-20 minutes. After incubation, cells were washed 3 times with PBS and staining media was changed with pre-warmed fresh RPMI media. Cells were imaged immediately at 579⁄599 nm excitation/emission.

3. RESULTS

3.1. Causal Variants for 2 Families Were Identified After Genetic Pre-screenings

Before sending DNA samples to whole exome sequencing, index cases and affected siblings were screened for population specific founder mutations and most commonly mutated genes for each disease group. Suggested genetic pre-screenings and laboratory pre-screenings for each disease group were given in **Table 2.15**. After genetic pre-screenings, causal variants for 2 families were identified as CLP1 c.419G>A; p.Arg140His and POMT1 c.598G>C; Ala200Phe **(Table 3.1)**.

Table 3.1 Variants identified after pre-screenings.

Proband	Sex	Disease Group	Gene	Coding impact	Zygosity	Transcript: Nucleotide; Protein
FMAL015.01	F	Muscular dystrophies and myopathies	POMT1	Missense	Homozygous	NM_007171.3: c.598G>C; Ala200Phe
FMAL038.01	M	Leukodystrophy	CLP1	Missense	Homozygous	NM_006831.3: c.419G>A; p.Arg140His

3.2. Causal Variants for 79 Families Were Identified After WES Data Analysis

After completing genetic pre-screenings, samples from families were sent to Broad Institute for whole exome sequencing. Whole exome sequencing was applied to 138 consanguineous families. By combining phenotypic data from PhenoTips platform, WES data analysis was carried out on RD-Connect platform using standard filtering criteria for rare diseases, including Minor Allele Frequency (MAF)<0.01, Variant Effect Predictor (VEP)=moderate/high and Combined Annotation Dependent Depletion (CADD) >20.

28 known variants in known disease genes **(Table 3.1)**, 32 novel candidate variants in known disease genes **(Table 3.2)** and 15 candidate disease genes **(Table 3.3)** were identified with an overall causative genetic defect identified in 57% of consanguineous families studied.

Table 3.1 Known variants identified in known disease genes.

Proband	Sex	Disease Group	Gene	Coding impact	Zygosity	Transcript: Nucleotide; Protein
FIZM002.01	F	Brain malformations	PORCN	Nonsense	Heterozygous de novo XLD	NM_203475.2: c.283C>T; p.Arg95Ter / Wild type
FDIY001.01	M	Brain malformations	VPS13B	Splice site	Compound heterozygous	NM_017890.4: c.412+1G>T NM_017890.4: c.7504+40A>T
FMAL011.01	F	Brain malformations	OCLN + MCCC2	Frameshift, Missense	Homozygous	NM_002538.3: c.173_194del ;p.Trp58PhefsTer10 NM_022132.5: c.1015G>A; p.Val339Met
FDIY011.01	F	ID with epilepsy	CDKL5	Missense	Heterozygous de novo XLD	NM_003159.2: c.587C>T; p.Ser196Leu / Wild type
FDIY032.01	M	Cerebellar hypoplasia or atrophy	FOLR1	Nonsense	Homozygous	NM_016725.2: c.610C>T; p.Arg204Ter
FDIY038.01	M	ID without epilepsy	MAN1B1	Missense	Homozygous	NM_016219.5: c.1000C>T; p.Arg334Cys
FIZM018.01	M	ID without epilepsy	MED12	Frameshift	Hemizygous	NM_005120.3: c.5898dupC; p.Ser1967GlnfsTer84
FIZM019.01	F	ID with epilepsy	PNPO	Missense	Homozygous	NM_018129.3: c.674G>A; p.Arg225His
FMAL026.01	F	Spastic paraplegia	ALS2	Missense	Homozygous	NM_020919.4: c.470G>A; p.Cys157Tyr
FMAL042.01	F	Spastic paraplegia	SACS	Nonsense	Homozygous	NM_014363.6: c.2182C>T; p.Arg728Ter
FMAL049.01	M	Spastic paraplegia	ALS2	Frameshift	Homozygous	NM_020919.4: c.4573dupG; p.Val1525GlyfsTer17
FMAL050.01	F	Muscular dystrophies and myopathies	CLCN1	Missense	Homozygous	NM_000083.2: c.1063G>C; p.Gly355Arg
FMAL052.01	F	Muscular dystrophies and myopathies	SGCA	Missense	Homozygous	NM_000023.4: c.850C>T; p.Arg284Cys
FMAL053.01	M	Leukodystrophy	ATP8A2	Nonsense	Homozygous	NM_016529.6: c.1756C>T; p.Arg586Ter
FMAL055.01	F	Spastic paraplegia	SPG11	Frameshift	Homozygous	NM_025137.4: c.3075dupA; p.Glu1026ArgfsTer4
FMAL065.01	M	Muscular dystrophies and myopathies	ETFDH	Missense	Homozygous	NM_004453.3: c.1130T>C; p.Leu377Pro
FMAL073.01	F	Spinocerebellar ataxias	CACNB4 + GSS	Missense, Splice site	Homozygous	NM_000726.4: c.8C>T; p.Ser3Phe NM_000178.4: c.834+4G>C
FMAL007.01	M	Leukodystrophy	CLP1	Missense	Homozygous	NM_006831.3: c.419G>A; p.Arg140His
FIZM029.01	M	ID with epilepsy	WWOX	Missense	Homozygous	NM_016373.4: c.689A>C; p.Gln230Pro
FMAL068.01	M	Muscular dystrophies and myopathies	NDUFAF6	Splice site	Homozygous	NM_001354533.1: c.259-3C>A
FIZM015.01	F	Brain malformation	CASK	Missense	Heterozygous de novo XLD	NM_003688.3: c.1910G>A; p.Gly637Asp / Wild type
FMAL031.01	F	Leukodystrophy	STAMBP	Missense	Homozygous	NM_201647.3: c.188A>G; p.Tyr63Cys
FDIY017.01	M	ID with epilepsy	ADSL	Missense	Homozygous	NM_000026.4: c.1288G>A; p.Asp430Asn
FMAL044.01	F	Muscular dystrophies and myopathies	SH3TC2	Frameshift	Compound heterozygous	NM_024577.3: c.1897delG; p.Ala633ProfsTer12 / NM_024577.3: c.1747_1748delAG; p.Arg583AlafsTer4
FMAL047.01	F	CMT and hereditary neuropathies	GDAP1	Frameshift	Homozygous	NM_018972.3 : c.786delG; p.Phe263LeufsTer22
FMAL041.01	M	ID without epilepsy	ERCC6	Splice site	Homozygous	NM_000124.4: c.1992+3A>G
FMAL002.01	M	Leukodystrophy	TACO1	Frameshift	Homozygous	NM_016360.4: c.472dupC; p.His158ProfsTer8
FMAL019.01	M	Leukodystrophy	SAMHD1	Nonsense	Homozygous	NM_015474.3: c.490C>T; p.Arg164Ter
FMAL017.01	M	Other phenotype	SAMHD1	Nonsense	Homozygous	NM_015474.3: c.490C>T; p.Arg164Ter

Table 3.2 Novel variants identified in known disease genes.

Proband	Sex	Disease Group	Gene	Coding impact	Zygosity	Transcript: Nucleotide; Protein
FIZM012.01	M	Muscular dystrophies and myopathies	NDUFA12	Frameshift	Homozygous	-
FIZM021.01	M	Brain malformation	GALK1	Missense	Homozygous	-
FIZM024.01	F	Brain malformation	LAMB1	Missense	Homozygous	-
FIZM027.01	F	Muscular dystrophies and myopathies	CACNA1S	Missense	Homozygous	-
FMAL009.01	F	Spinocerebellar ataxias	PRKCG	Missense	Homozygous	-
FMAL014.01	M	Muscular dystrophies and myopathies	COL12A1	Missense	Heterozygous de novo	-
FMAL024.01	M	Muscular dystrophies and myopathies	COLQ	Nonsense	Homozygous	-
FMAL027.01	F	Muscular dystrophies and myopathies	ISPD	Splice site	Homozygous	-
FDIY014.01	M	Mitochondrial disorders	GAMT	Frameshift	Homozygous	-
FDIY015.01	F	ID with epilepsy	FOXRED1	Missense	Homozygous	-
FDIY021.01	M	Brain malformation	HADH	Synonymous	Homozygous	-
FDIY023.01	M	Brain malformation	TAF1	Missense	Hemizygous	-
FDIY024.01	M	Leukodystrophy	COL4A1	Missense	Homozygous	-
FIZM014.01	F	CMT and hereditary neuropathies	TBCD	Missense	Homozygous	-
FIZM007.01	M	CMT and hereditary neuropathies	DPAGT1	Missense	Homozygous	-
FIZM016.01	M	ID with epilepsy	ARX	Splice site	Hemizygous	-
FIZM020.01	F	Mitochondrial disorders	RMND1	Missense	Homozygous	-
FMAL029.01	M	ID with epilepsy	DENND5A	Nonsense	Homozygous	-
FMAL061.01	M	Brain malformation	STIL	Nonsense	Homozygous	-
FMAL070.01	M	ID with epilepsy	AP3B2	Frameshift	Homozygous	-
FMAL071.01	M	ID with epilepsy	SPTBN2	Frameshift	Homozygous	-
FMAL072.01	F	ID with epilepsy	PCDH12	Nonsense	Homozygous	-
FMAL076.01	M	ID with epilepsy	PIGT	Missense	Homozygous	-
FMAL033.01	M	ID without epilepsy	RNASET2	3 prime UTR	Homozygous	-
FIZM010.01	F	Brain malformations	TLK2	Missense	Homozygous	-
FMAL012.01	F	ID with epilepsy	CC2D1A	Splice site	Homozygous	-
FMAL039.01	M	CMT and hereditary neuropathies	SLC39A8	Missense	Homozygous	-
FMAL016.01	F	Brain malformation	KATNB1	Missense	Homozygous	-
FIZM032.01	M	ID without epilepsy	SNX14	Nonsense	Homozygous	-
FDIY018.01	F	Brain malformations	TCF20	Missense	Heterozygous de novo	-

Table 3.2 Novel variants identified in known disease genes (Continued)

Proband	Sex	Disease Group	Gene	Coding impact	Zygosity	Transcript: Nucleotide; Protein
FDIY0039.01	M	ID with epilepsy	WWOX	Missense	Homozygous	-
FIZM006.01	M	ID with epilepsy	WWOX	Missense	Homozygous	-
FMAL028.01	M	ID with epilepsy	WWOX	Missense	Homozygous	-
FMAL058.01	F	ID with epilepsy	ADSL	Missense	Homozygous	-
FIZM022.01	M	ID with epilepsy	ADSL	Missense	Homozygous	-

Table 3.4 Variants identified in novel candidate genes.

Proband	Sex	Disease Group	Gene	Coding impact	Zygosity	Transcript: Nucleotide; Protein
FIZM011.01	M	Brain malformations	-	Missense	Homozygous	-
FMAL023.01	F	Leukodystrophy	-	Missense	Homozygous	-
FIZM026.01	M	Muscular dystrophies and myopathies	-	Missense	Homozygous	-
FDIY026.01	M	ID with epilepsy	-	Missense	Homozygous	-
FDIY028.01	F	Brain malformations	-	Missense	Homozygous	-
FDIY030.01	F	Brain malformations	-	Missense	Homozygous	-
FMAL034.01	M	Muscular dystrophies and myopathies	-	Missense	Homozygous	-
FMAL077.01	M	ID with epilepsy	-	Nonsense	Homozygous	-
FMAL078.01	M	ID with epilepsy	-	Missense	Homozygous	-
FMAL079.01	M	ID with epilepsy	-	Missense	Homozygous	-
FMAL022.01	M	Spinocerebellar ataxias	-	Missense	Homozygous	-
FMAL035.01	M	Brain malformations	-	Nonsense	Homozygous	-
FMAL051.01	M	ID with epilepsy	-	Nonsense	Homozygous	-
FMAL057.01	F	Leukodystrophy	-	Splice site	Homozygous	-
FDIY022.01	M	Brain malformations	-	Missense	Homozygous	-

3.3. Identified Variants Were Grouped According to Detection Rate

After applying WES to 138 consanguineous families, novel variants in known disease genes were identified in 35 families, known variants in known disease genes were identified in 29 families and novel candidate genes potentially involved in the development of neurogenetic conditions were identified in 15 families. Among the families with novel and known variants in known disease genes, novel inheritance mode and double trouble were identified in 2 families and expanded phenotype was identified in 3 families. Additionally, 8 of them solved with potential founder mutations in Turkish population. In overall, potential molecular causes were identified in 57% of families and 59 of the cases are still unsolved **(Figure 3.1)**.

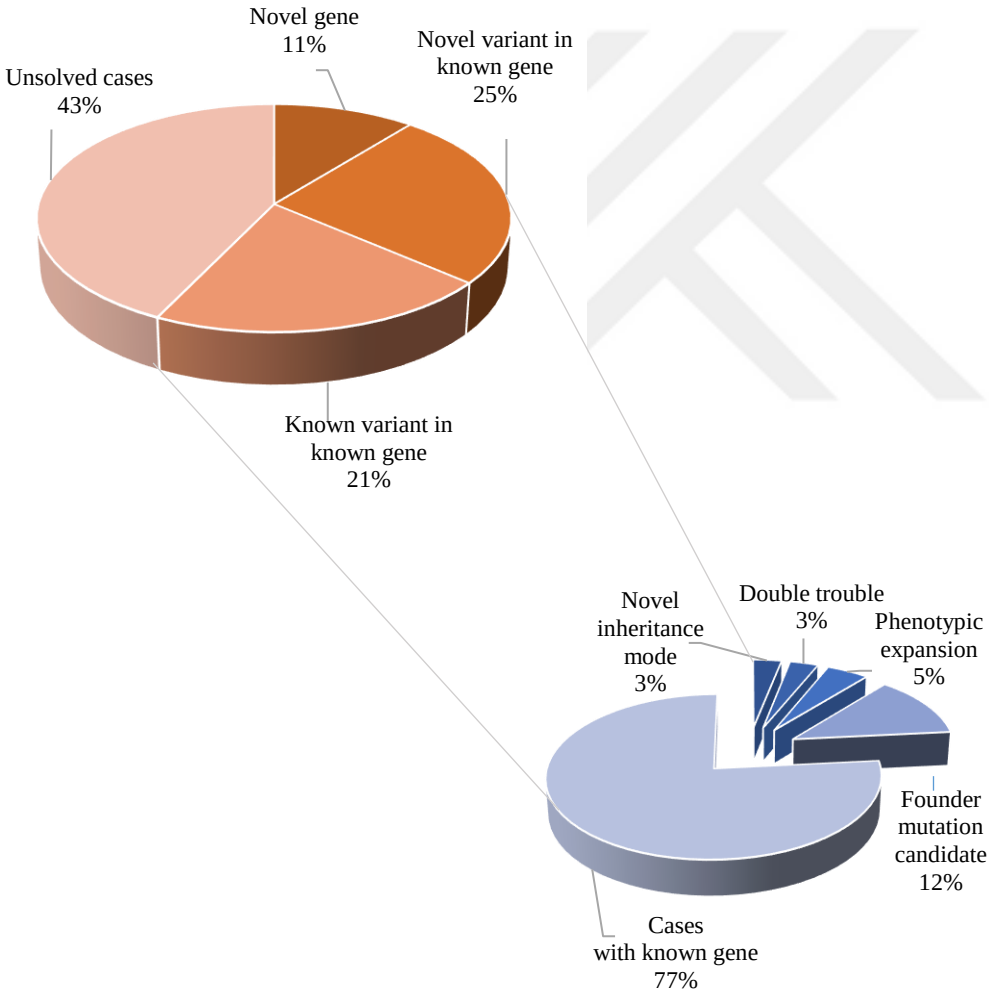

Figure 3.1 Summary of findings from WES according to detection rate. Analysis of data from WES revealed families with known variants in known genes in 21%, novel variants in known genes in 25%, novel candidate genes in 11% of the families, Among the families with novel and known variants in known disease genes, potential founder mutation candidates in 12%, phenotypic expansion in 5%, novel inheritance in 3% and double trouble in 3% of the families were identified.

3.2. Identified Variants Were Grouped According to Inheritance Mode

We have also grouped variants according to their mode of inheritance. 70 of the families showed autosomal recessive inheritance in homozygous state, 2 families showed autosomal recessive inheritance in compound heterozygous state and 2 families showed X-linked recessive inheritance in hemizygous state for a causal variant. Additionally, 2 families were genetically diagnosed with de novo autosomal dominant variants and 3 families with de novo X-linked dominant variants in heterozygous state.

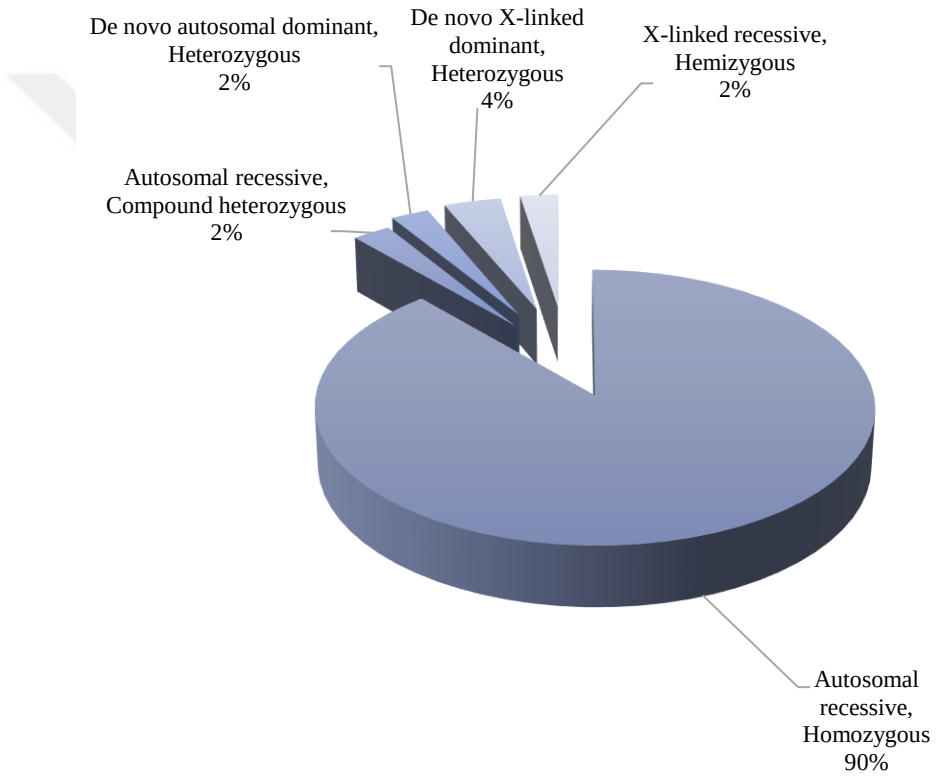

Figure 3.2 Summary of findings from WES according to inheritance mode Analysis of data from WES revealed homozygous variants with autosomal recessive transmission in 90%, compound heterozygous variants with autosomal recessive transmission in 2%, hemizygous variants with X-linked recessive transmission in 2%, de novo autosomal dominant variants in 2%, de novo X-linked dominant variants in 4% of the families.

3.3. Genetic Diagnosis Success Rates by Disease Groups

We next wanted to compare genetic diagnosis success rates between disease groups. After completing genetic pre-screenings and WES data analysis, we showed that causal variants for 17 families out of 21 from brain malformations group, 9 families out of 15 from leukodystropy group, 2 families out of 3 from mitochondrial disorders group, 4 families out of 9 from CMT and hereditary neuropathies, 4 families out of 5 from spastic paraplegia group, 3 families out of 4 from spinocerebellar ataxia group, 5 families out of 16 from intellectual disability without epilepsy group, 22 families out of 43 from intellectual disability with epilepsy group, 13 families out of 20 from muscular dystrophy and myopathy group, 1 family out of 1 from cerebellar hypoplasia or atrophy group and 1 family out of 3 from other phenotype group were genetically diagnosed.

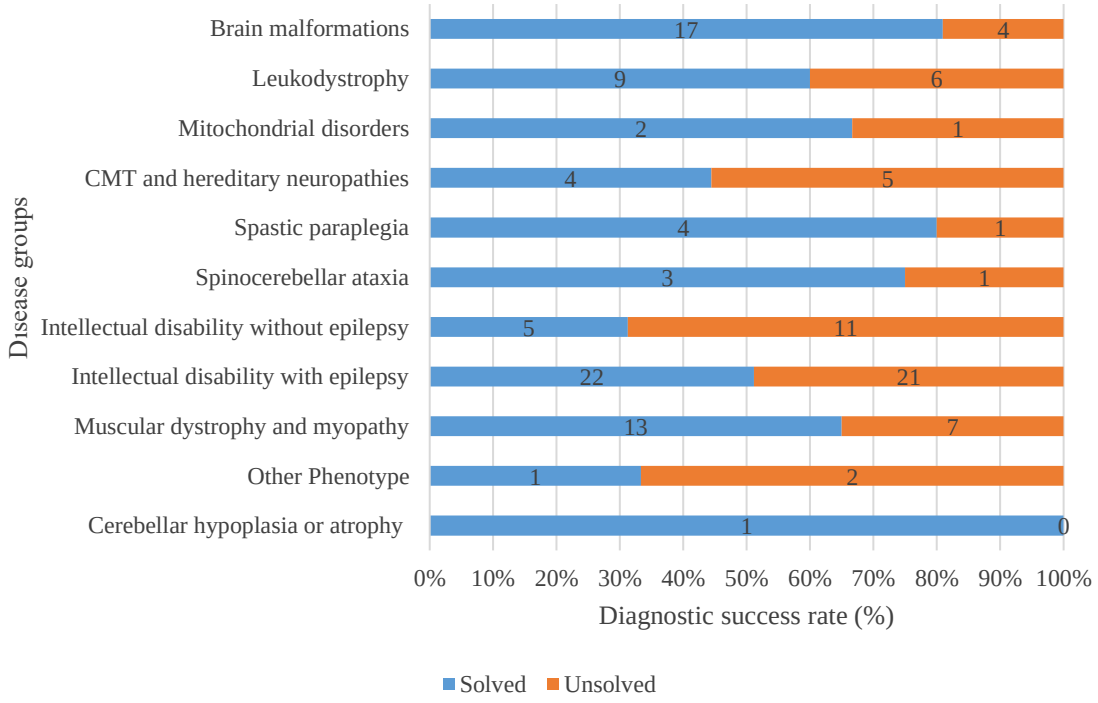

Figure 3.3 Summary of diagnostic success rates according to disease groups. Genetic diagnosis success rates were identified in brain malformations group (81%), leukodystrophy group (60%), mitochondrial disorders group (67%), CMT and hereditary neuropathy group (45%), spastic paraplegia group (80%), spinocerebellar ataxia group (75%), intellectual disability without epilepsy (40%) and intellectual disability with epilepsy groups (53%), muscular dystrophy and myopathy group (69%), cerebellar hypoplasia or atrophy group (100%) and other phenotype group (34%) after genetic pre-screenings and WES data analysis.

3.4. Identified Variants Were Grouped According to Their Subcellular Localization

In order to see where protein products of identified genes function inside the cell, we grouped identified genes according to their subcellular localizations. Among the 80 identified genes from genetic pre-screenings and WES data analysis, 12 of them function in cytoplasm, 13 of them function in plasma membrane and channels, 14 of them function in mitochondria, 6 of them function in cytoskeleton and microtubules, 7 of them function in endoplasmic reticulum, 14 of them function in nucleus, 6 of them function in extracellular space, 4 of them function in endosome and 4 of them function in Golgi apparatus.

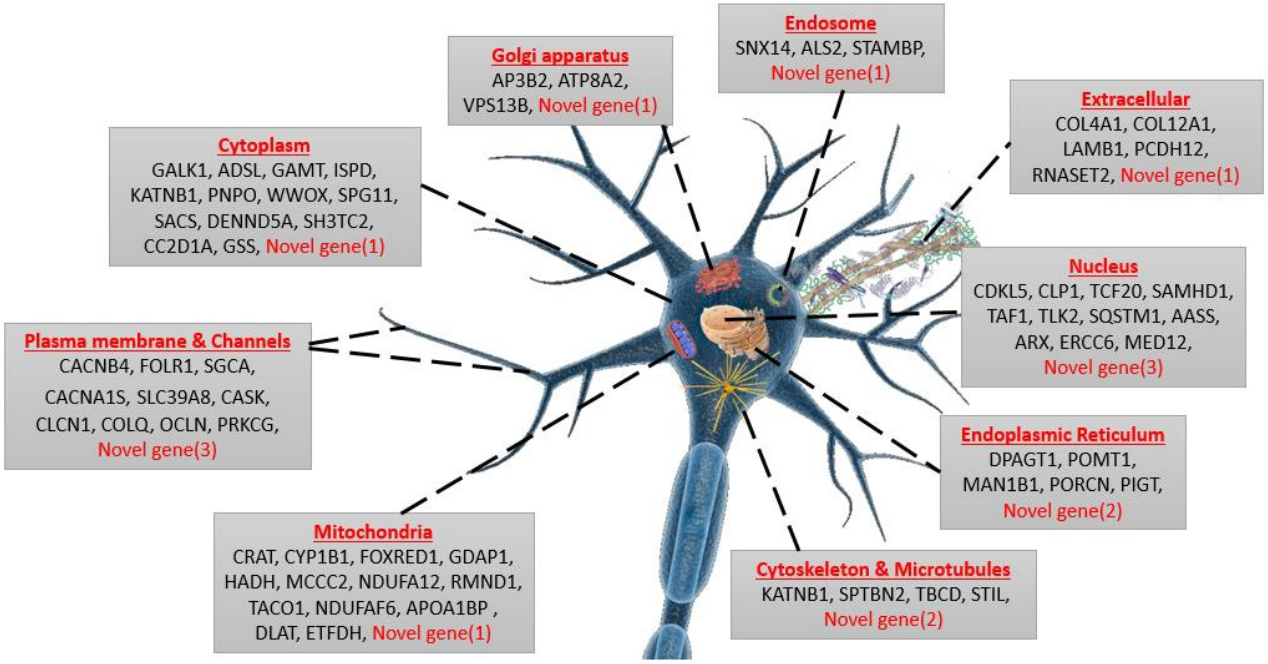

Figure 3.4 Schematic showing of subcellular localization of the protein products of identified genes. Grouping identified genes according to their subcellular localization revealed nine major groups: cytoplasm (15%), mitochondria (17%), cytoskeleton and microtubules (8%), endoplasmic reticulum (9%), nucleus (17%), extracellular space (8%), Golgi apparatus (5%), plasma membrane and channels (16%) and endosome (5%).

3.5. PTPMT1 Was Identified As Mitochondrial Candidate Causal Gene Responsible For the Development of Neurogenetic Conditions

After performing WES data analysis, candidate causal gene for a family which is initially diagnosed as brain malformation was identified as Protein Tyrosine Phosphatase, Mitochondrial 1 (PTPMT1) gene. Variant (c.255G>C; p.Gln85His) with 24.8 CADD score, damaging predictions in SIFT and MutationTaster (MT) web tools and possibly damaging prediction in PolyPhen2 (PP2) web tool is a missense variant in the splice region. Segregation analysis of the variant between affected proband and unaffected parents was done by Sanger sequencing. Both unaffected parents were carriers for the variant identified in the proband.

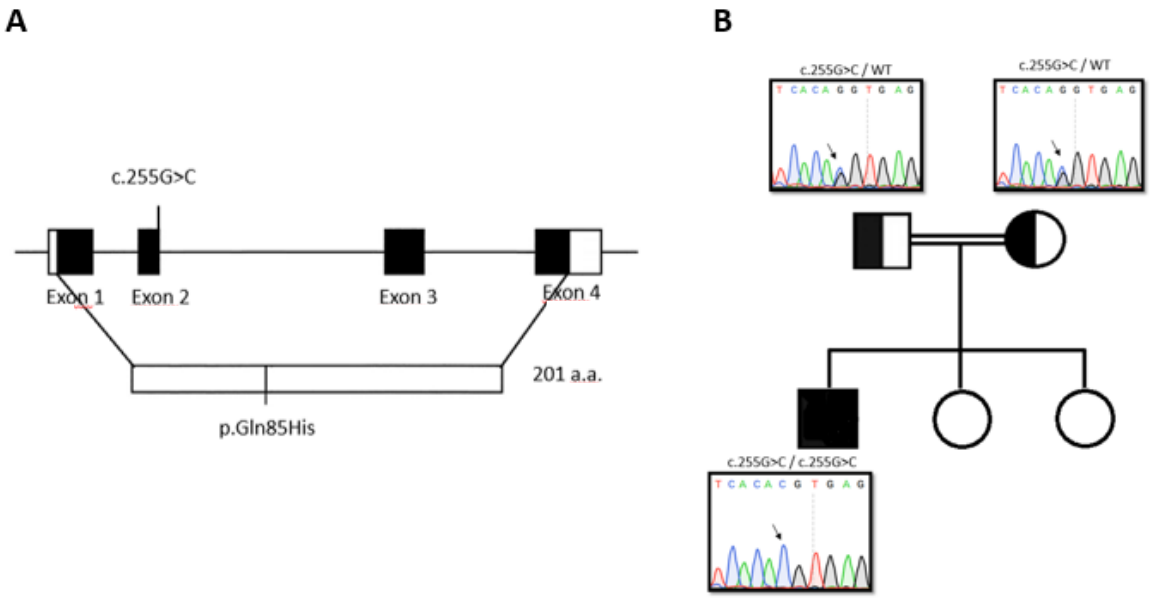

Figure 3.5 PTPMT1 gene structure and segregation of a variant in the family. (A) Schematic representation of PTPMT1 c.255G>C variant on the gene and its protein product. **(B)** The presence and segregation of PTPMT1 c.255G>C variant was validated by Sanger sequencing. Both parents are heterozygous and proband is homozygous for the variant.

3.6. Sequencing of cDNA in Patient with a PTPMT1 c.255G>C Variant Revealed Defect in Pre-mRNA Splicing

To see the effect of the 5'splice donor site variant (c.255G>C) on the pre-mRNA splicing, we first obtained skin biopsy sample from the patient and produced primary patient fibroblasts. cDNA was produced from the isolated RNA and PTPMT1 cDNA sequence was amplified on full-length cDNA template. Sequencing of PTPMT1 cDNA revealed an insertion of 162 bp from the 5'intronic part, skipping of exon 3 and formation of premature stop codon inside the intronic portion.

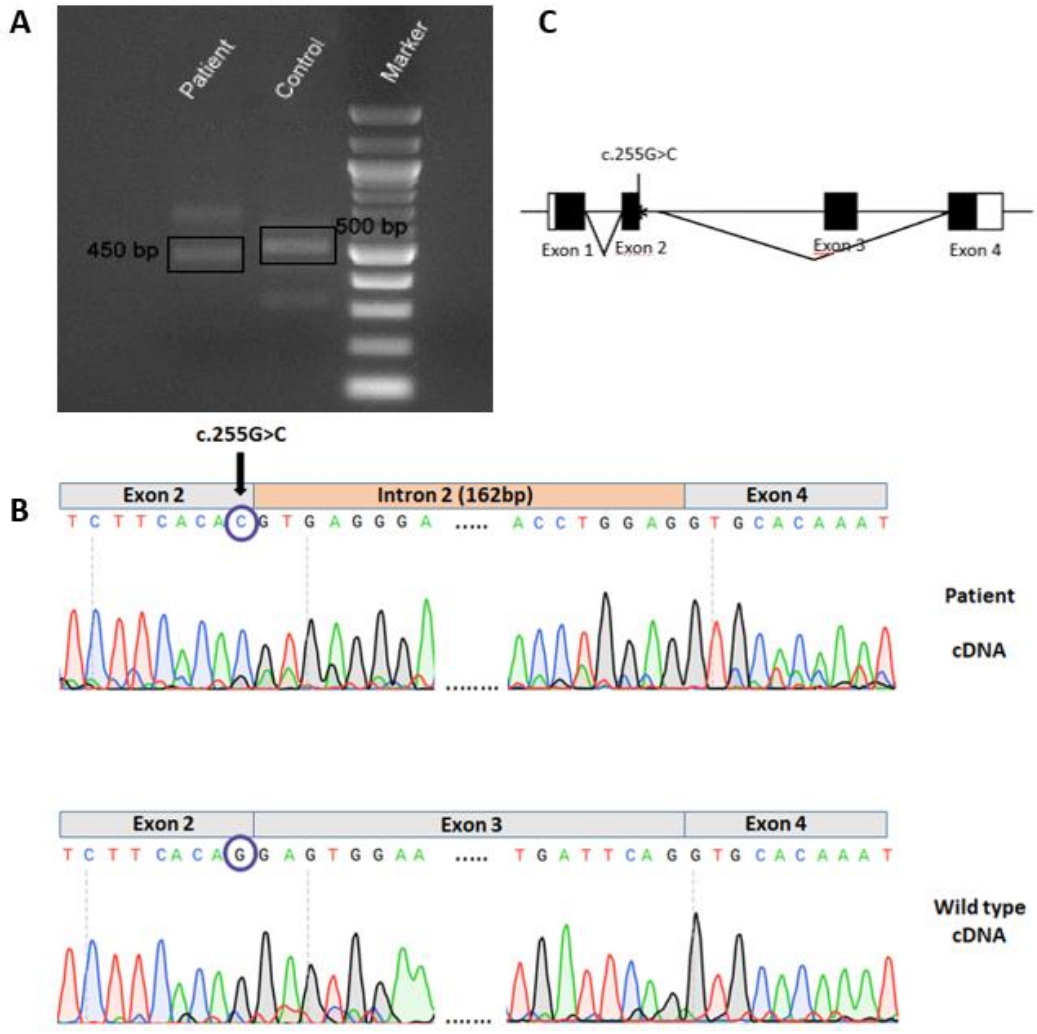

Figure 3.6 Analysis of the c.255G>C variant effect on pre-mRNA splicing. (A) RT-PCR products of control and patient cDNA amplified with primers spanning exon 1 and exon 4 on 1.5% agarose gel. The black rectangles show the eluted bands used for sequencing afterwards **(B)** Sanger sequencing of PCR products from patient and control shows insertion from intron 2 and skipping of exon 3 in patient. **(C)** Schematic representation of the splicing defect caused by PTPMT1 c.255G>C variant.

3.7. Western Blot Analysis of PTPMT1 Protein Expression Revealed the Absence of Protein Expression

After showing the formation of premature stop codon by Sanger sequencing of patient cDNA, we checked the expression of PTPMT1 protein by Western blot. Firstly, we isolated total protein from patient fibroblasts and two different control fibroblasts, then compared PTPMT1 protein expression between patient and control groups. Western blot revealed no expression of PTPMT1 protein in the patient. B-actin was used as a reference for positive control

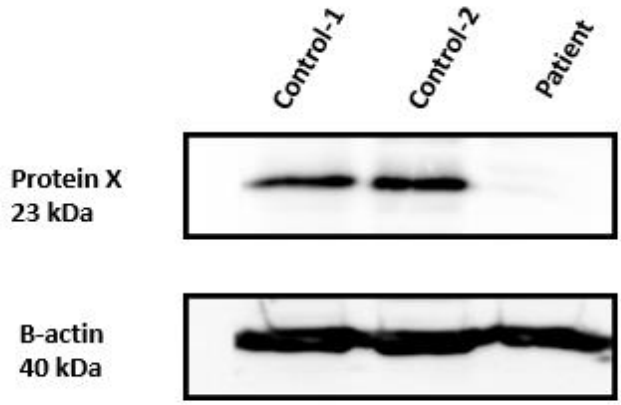

Figure 3.7 Western blot analysis of PTPMT1 protein expression. Western blot analysis revealed no protein product in the patient fibroblast. B-actin was used as a loading control.

3.8. Blue-Native Polyacrylamide Gel Electrophoresis (BN-PAGE) Revealed Unchanged Assembly of OXPHOS Components in Patient Fibroblasts

In order to see the effect of the absence of PTPMT1 protein expression on OXPHOS components assembly, mitochondria were isolated from the patient fibroblasts and OXPHOS components were purified from mitochondrial inner membrane. Blue-native gel electrophoresis (3-12% gradient) and western blot analysis of the isolated complexes from patient fibroblasts revealed no change in the amount of assembled complexes when compared with sex and age-matched control.

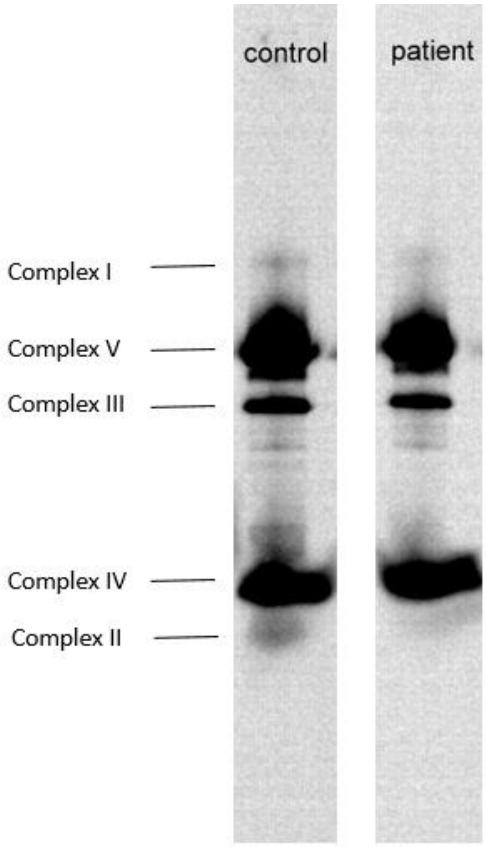

Figure 3.8 Blue-native polyacrylamide gel electrophoresis (BN-PAGE) analysis of assembly of OXPHOS components in patient with homozygous PTPMT1 variant. One-dimensional BN-PAGE and the immunoblotting of individual OXPHOS complexes of the patient reveal no change in the assembly of OXPHOS complexes. OXPHOS complexes were detected by using antibody cocktail including complex specific antibodies (Complex I-NDUFA9, Complex II- 70 kDa SDHA, Complex III-core protein UQCRC2, Complex IV-COX IV and Complex V-alpha subunit ATP5A).

3.9 Patient Fibroblasts with the Homozygous PTPMT1 Variant Showed Disorganized Mitochondrial Network

Here we checked the mitochondrial morphology and membrane potential by staining control and patient fibroblasts with MitoTracker Red CMXRos red-fluorescent dye and Hoechst 33342. Control fibroblasts showed long, tubular and intact mitochondrial morphology and continuous mitochondrial network **(Figure 3.9A)**. Whereas, patient fibroblasts showed smaller, fragmented and rounded mitochondrial morphology with non-continuous mitochondrial network **(Figure 3.9B)**. Additionally, patient fibroblasts showed reduced mitochondrial membrane potential with lower red fluorescent signal.

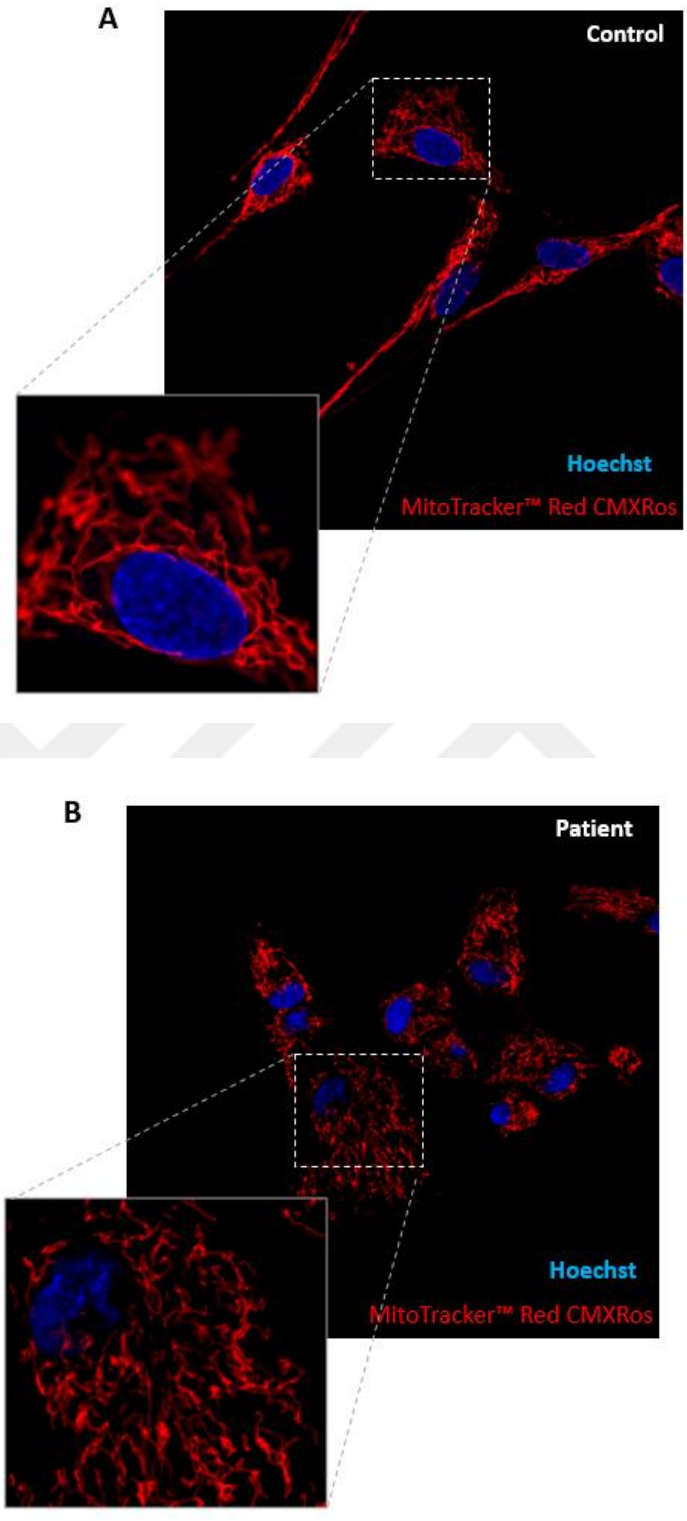

Figure 3.9 Representative confocal microscopy images of patient fibroblasts stained with Mitotracker Red CMXRos and Hoechst 33342. Control and patient fibroblasts were stained with 100 nM with Mitotracker Red CMXRos and 1 µg Hoechst 33342 dyes. **(A)** Control fibroblasts with long, tubular mitochondria and continuous mitochondrial network **(B)** Patient fibroblasts with rounded and fragmented mitochondria and non-continuous mitochondrial network

4. DISCUSSION

Consanguineous marriages constitute more than 10% of all marriages worldwide (Bittles & Black, 2010). Marriage between relatives is also frequent in Turkey (~25%) and they are associated with an increased risk of genetic conditions inherited autosomal recessively (Kaplan et al., 2016). Neurogenetic conditions that affect the development and function of brain, muscles and nervous system can lead to severe disabilities and premature mortality. Since the early 21st century, development in the field of neurogenetics generated a large number of genetically defined neurogenetic disease entities which are collectively resulting in a considerable public health and economic problems. Today, next-generation sequencing enables early identification of treatable cases even before severe, disease-specific symptoms occur, explains pathophysiology behind neurogenetic diseases and simplifies the "diagnostic odyssey" of patients (Keogh & Chinnery, 2013).

Although they are individually rare, there are approximately 7000 inherited rare diseases affecting about 350 million people in the world and only half of them are molecularly characterized. According to a report published in 2016 by the Turkish Statistical Institute (TUIK), rare diseases affect 5-6 million people in Turkey (Sarıkaya, 2018). In 2009, WES firstly diagnosed a patient with homozygous mutation in SLC26A3 gene associated with chloride diarrhea. Over the last few years, Whole exome sequencing has shown huge success in discovering causal variants in rare diseases by overcoming limitations of linkage analysis (Tetreault, Bareke, Nadaf, Alirezaie, & Majewski, 2015). So, WES contributed a lot to research field and clinical diagnosis.

In our study, three pediatric neurology clinics in Izmir, Malatya and Diyarbakir were selected as centers from different geographical regions of Turkey to recruit patients as part of the CONSEQUITUR project. Consanguineous families with children who have one of the childhood neurogenetic diseases were included in the study. Patients were grouped into 11 major disease groups (Intellectual disability with epilepsy, intellectual disability without epilepsy, brain malformation, leukodystrophy, spinocerebellar ataxia, spastic paraplegia, CMT and hereditary neuropathy, muscular dystrophy and myopathy, mitochondrial disorders, cerebellar hypoplasia or atrophy and other phenotypes) according to initial clinical manifestations. In the frame of this project, 199 consanguineous families were recruited and 61 of them have more than one affected children.

Standardized phenotypic data collection forms were used for deep phenotyping of affected individuals. Phenotype forms with different contents were generated for different disease groups. Phenotypic data including developmental data, physical examination, laboratory investigations, genetic tests and investigations were recorded by using standardized Human Phenotype Ontology (HPO) terms via PhenoTips software to enable the data to be read by the computer softwares and combined with the RD-Connect and the other project data sets. So, accurate and consistent phenotypic characterization of neurogenetic conditions affecting consanguineous families in Turkey expanded the knowledge on genotype-phenotype correlations as the basis for further researches.

Prior to WES, disease category specific genetic, laboratory and clinical prescreening tests were performed by collaborating with Newcastle University. Before inclusion of patients in the study, in addition to laboratory and clinical prescreening tests, some genetic prescreening tests for disease specific most commonly seen genes and founder mutations were performed at clinical evaluation stage. After showing that patients are negative for specific mutations, they were included in the study and blood samples were obtained from each family member to perform whole exome sequencing.

In our laboratory, CLP1 (Cleavage and Polyadenylation Factor I Subunit) founder mutation c.419G>A, p.Arg140His was screened by Sanger sequencing for intellectual disability, leukodystrophy, Charcot-Marie-Tooth (CMT) hereditary neuropathy and cerebellar hypoplasia or atrophy disease categories. CLP1 is a kinase involved in the maturation of tRNA, mRNA and siRNA. Any defect in CLP1 gene leads to destabilization of tRNA endonuclease complex (TSEN), impaired cleavage of pre-tRNA and defects in brain development (Schaffer et al., 2014). At the end of CLP1 prescreening tests, we identified one family with CLP1 c.419G>A, p.Arg140His founder mutation.

In Newcastle University, during prescreening tests, another founder mutation c.598G>C p.Ala200Pro in POMT1 (protein O-mannosyltransferase 1) gene was identified in one family. POMT1 prescreening test was performed for congenital or childhood-onset muscular dystrophy and myopathy disease group. POMT1 is an O-mannosyltransferase located in the endoplasmic reticulum (ER) and used in O-mannosylation of proteins. Walker-Warburg syndrome (WWS) and limb-girdle muscle dystrophy type 2K (LGMD2K) are most common diseases resulted from the defects in this gene (Balci et al., 2005).

So, initially performed single or multigene prescreening tests for relevant disease groups **(given in Table 2.15)** identified causal variants in two families prior to WES. Genetic prescreening tests to detect mutations in disease relevant genes at disease stage or prior to disease onset provide cost-effective and time-saving diagnosis of diseases, appropriate clinical management and patient specific treatment options (Dinh et al., 2011).

To date, we applied whole exome sequencing to 640 individuals belonging to 138 different families. We identified disease causing and potentially disease-causing variants in 79 of them. Among them, novel variants in known disease genes were identified in 35 families, known variants in known disease genes were identified in 29 families and novel candidate genes potentially involved in the development of neurogenetic conditions were identified in 15 families. WES analysis in patients with childhood hereditary neurological disorders revealed 57.24% diagnostic yield which is higher than the average diagnostic rate of previous studies in large cohorts with neurogenetic disorders (Fogel, Satya-Murti & Cohen, 2016). Current diagnostic yield in analyzed large cohorts is 25-40% (Robinson, Piro, & Jäger, 2017).

Identification of potentially disease causing novel variants and genes increases the establishment of knowledge on genotype-phenotype correlation in specific disease groups. Among families solved with novel variants in known disease genes and known variants in known disease genes, two of them are “double trouble” cases (brain malformation group / OCLN (Occludin)+MCCC2 (Methylcrotonoyl-CoA carboxylase 2) and spinocerebellar ataxia group / CACNB4(Calcium Voltage-Gated Channel Auxiliary Subunit Beta 4) +GSS (Glutathione synthetase)) with variants in two different genes suggested as disease causing. So, exome sequencing lightened the two cases with severe phenotypes caused by pathogenic variants in two different neurogenetic disease related genes and reduced the diagnostic challenge.

Besides that, WES identified two cases with novel inheritance pattern in two genes (spinocerebellar ataxia group/PRKCG (Protein Kinase C Gamma) and brain malformation group/TLK2 (Tousled Like Kinase 2)) which are usually inherited in autosomal dominant manner. WES analysis identified homozygous missense variants in index cases and affected siblings, while heterozygous missense variants in unaffected parents (Koht et al., 2012; Reijnders et al., 2018; Van De Warrenburg et al., 2003; Yabe et al., 2016). So, our data provides new insights into evaluations of challenging families with similar clinical phenotypes.

Our findings also broadened the phenotypic spectrum of several genes associated with neurogenetic conditions. Especially for the rare syndromes, it is important to fully explain clinical spectrum for accurate diagnosis (Schwartz et al., 2018).

Additionally, WES data analysis identified 4 potential founder mutations in Turkish population. These are still candidates for being founder mutation because haplotype analysis is required to confirm possible founder effect of identified variants. First candidate is homozygous frameshift TACO1 (Translational Activator of Cytochrome C Oxidase I) c.472dupC; p.His158ProfsTer8 which is previously described in another Turkish family with similar clinical findings. Second candidate is rare homozygous stop-gain SAMHD1 (SAM and HD Domain Containing Deoxynucleoside Triphosphate) c.490C>T; p.Arg164Ter variant which is identified in two different families in this study. Third candidate is novel homozygous missense WWOX (WW Domain Containing Oxidoreductase) c.716T > G; p.Leu239Arg variant which is identified in 3 different families in this study and 4 additional families from different centers across the Turkey. Other potential founder mutation candidate is rare homozygous missense ADSL (Adenylosuccinate Lyase) c.268G>A; p.Ala90Thr that is identified in 2 different families in our study.

When identified variants are grouped according to their mode of inheritance, among investigated 79 consanguineous families, autosomal recessive inheritance in homozygous (70) and compound heterozygous state (2), X-linked recessive inheritance in hemizygous state (2), de novo autosomal dominant variants (2) and de novo X-linked dominant variants in heterozygous state (3) were detected. Due to higher probability of inheriting identical copies of damaging recessive genes from a common ancestor, autosomal recessive inheritance in 92% of the families was an expected percentage in our large consanguineous Turkish cohort.

When we compare genetic diagnosis success rates between disease groups determined according to initial manifestations of diseases **(Figure 3.3)**, diagnostic success rates in brain malformation (81%), spastic paraplegia group (80%), spinocerebellar ataxia group (75%), muscular dystrophy and myopathy group (69%) and mitochondrial disorders group (67%) are higher. Disease group with the lowest diagnostic success rate is intellectual disability without epilepsy (40%) group. So, as in previous studies, genetic diagnosis was mostly achieved in neurogenetic disease groups with severe, specific phenotype rather than cases with isolated abnormalities (Trujillano et al., 2017).

Grouping of identified genes according to cellular compartment where they function revealed accumulation of genes mostly in nucleus, cytoplasm, plasma membrane/channels and mitochondria. In our cohort, mitochondrial etiology behind the cases which are initially diagnosed as pure neurological conditions is higher than expected. Because, neurological symptoms of the brain, muscles, and peripheral nervous system considerably overlapping with other hereditary neurological disorders are the most prevalent clinical presentations of mitochondrial disorders due to critical mitochondrial ATP demand of neurons. So, phenotypic and genotypic heterogeneity of mitochondrial disorders lead challenges in genetic diagnosis (Kumar, 2016). Clinicopathological characteristics and prognosis of these conditions indicate that pathways related mitochondrial dysfunction may be more prevalent in development of neurodegenerative disease. In this cohort, we identified 13 causal variants in NDUFA12, FOXRED1, TACO1, RMND1, ETFDH, HADH, CRAT, CYP1B1, GDAP1, MCCC2, NDUFAF6, APOA1BP, DLAT genes that are essential for normal mitochondrial function and 1 novel candidate gene PTPMT1 with a mitochondrial mechanism.

At the end of WES data analysis, we most importantly identified currently treatable cases such as families with variants in FOLR1, GAMT, GALK1 and ETFDH genes.

Although its huge contribution to causal gene and variant identification, WES has some limitations. At the end of WES data analysis in our cohort, 59 families remained genetically unsolved. WES captures exomes, so there is no screening of introns and regulatory elements including promoter regions, enhancers and some cryptic splice sites. Additionally, due to the short-read sequencing strategy, WES has difficulty to detect structural variations (SVs) including CNVs, large deletions, insertions and translocations. So, any mutation in intronic and regulatory regions and structural variations cannot be detected by WES (Biesecker, Shianna, & Mullikin, 2011). In addition to this, elevated level of genetic heterogeneity and phenotypic overlapping in studied disease groups leads some challenges in prioritization of identified variants. Families without clear candidate causal variants will be comprehensively analyzed, taking into account already identified SNVs, InDels, CNVs. Whole Genome Sequencing (WGS) and transcriptome analysis will be applied to identify variants affecting regulatory regions, structural variants, splicing variants and affected biological pathways through transcript expression levels.

Through exome sequencing we have identified the causative genetic defect in 57% of the families including 15 novel candidate genes whose function in nervous system is largely

unknown. To understand pathways related with those genes and their impact on nervous system function, we will perform functional studies depending on the function of mutated gene. We will use induced neuronal progenitor cells (iNPCs) from patient fibroblasts as a tool to study tissue-specific effects of variants and genes in neurons, develop zebrafish models using CRISPR/Cas9 technology which is currently used in our lab to elucidate the neurodevelopmental impact of genetic defects and multi-omic analyses.

Here, I showed functional studies performed for one novel mitochondrial disease gene example PTPMT1 (Protein Tyrosine Phosphatase Mitochondrial 1) to explain its function in nervous system. PTPMT1 is a mitochondrial inner membrane localized lipid phosphatase that leads to dephosphorylation of phosphatidylglycerophosphate (PGP) to phosphatidylglycerol (PG). Previous studies showed the role of PTPMT1 in cardiolipin biosynthetic pathway, ATP and insulin production (Niemi, Lanning, Westrate, & Mackeigan, 2013). A few months ago, Zheng et al. showed that PTPMT1 knockout neural precursor/stem cells lead to inhibition of cerebellar and cerebral development in mice and decrease in mitochondrial pyruvate uptake and mitochondrial aerobic respiration (Zheng et al., 2018). This study gave us important clues about the role of PTPMT1 in nervous system development because phenotypic expressions of the mutation in mice show similarities with our patient's clinical findings. Neural precursor/stem cells specific PTPMT1 knockout mice shows growth retardation, ataxia, tremor, impaired motor coordination, thinner cerebral cortex, smaller hippocampus, larger ventricles and small cerebella with missing foliation and lamination. Similarly, our patient with PTPMT1 c.255G>C variant displays abnormality of the cerebellum as dysmetria, abnormal pyramidal signs as spasticity and hyperreflexia, motor delay, corpus callosum hypoplasia, mega cisterna magna.

PTPMT1 c.255G>C is a 5'splice donor site variant. To check splicing defect, primary patient fibroblasts were produced from skin biopsy sample. Sequencing of PTPMT1 cDNA revealed an insertion of 162 bp from the 5'intronic part, skipping of exon 3 and formation of premature stop codon inside the intronic portion. Western blot analysis of PTPMT1 protein expression revealed no expression of PTPMT1 protein in the patient fibroblasts.

To see the effect of the absence of PTPMT1 protein expression on OXPHOS components assembly, mitochondria were isolated from the patient fibroblasts and OXPHOS components were purified from mitochondrial inner membrane for Blue-Native gel electrophoresis. BN-PAGE revealed no change in the amount of assembled complexes. Actually, this was an

expected result because PTPMT1 does not directly join the structure of OXPHOS complexes. Previous studies demonstrated that PTPMT1 helps regulation of membrane integrity and organelle activity (Zhang et al., 2011). And, the complexes of OXPHOS can combine with each other to form structures called as supercomplexes (Signes & Fernandez-vizarra, 2018). So, we performed BN-PAGE to see whether there is any defect in assembly of OXPHOS supercomplexes because any defect in the maintenance of membrane integrity will affect the organization and assembly of OXPHOS supercomplexes. However, BN-PAGE also revealed no change in the supercomplex assembly.

Zhang et al. also examined the mitochondrial morphology using immunocytochemistry and showed fragmented mitochondria in Ptpmt1-deficient MEFs (Zhang et al., 2011). Then, we checked the mitochondrial morphology and membrane potential in primary patient fibroblasts with PTPMT1 c.255G>C variant by staining with MitoTracker Red CMXRos red-fluorescent dye. CMXRos red-fluorescent dye is cationic, lipophilic fluorescent dye which accumulates inside the mitochondria due to its negatively charge and its accumulation depends on the mitochondrial membrane potential (Pendergrass, Wolf, & Poot, 2004). Patient fibroblasts showed smaller, fragmented and rounded mitochondrial morphology with non-continuous mitochondrial network **(Figure 3.9B)** and reduced mitochondrial membrane potential with lower red fluorescent signal (data not shown). We showed the requirement of PTPMT1 in maintenance of mitochondrial fusion-fission processes and balanced mitochondrial network.

To see the tissue-specific effects of the PTPMT1 deficiency in neurons, we are optimizing the direct conversion protocol from Meyer et. al to generate induced neural progenitor cells (iNPCs) from primary patient fibroblasts by timely restricted overexpression of Oct4, Sox2, Klf4 and c-Myc together with neural induction media (Günther, Wörsdörfer, Meyer, Edenhofer, & Thier, 2015).

5. CONCLUSION

Neurogenetic disorders are dysfunctions of peripheral or central nervous systems and they are heterogeneous both genetically and phenotypically. Most of the neurogenetic disorders fall into rare disease category and their diagnosis is problematic due to insufficient understanding about these conditions. Here, we showed the clinical utility and high diagnostic yield of whole exome sequencing in the diagnosis of neurogenetic disorders.

Our study identified causal and potential causal variants in 79 out of 138 consanguineous families with >57% diagnostic yield. WES data analysis revealed 32 novel variants in known disease genes, 28 known variants in known disease genes, 15 candidate disease genes and 4 candidate founder mutations.

To the best of our knowledge, this is the largest comprehensive genomic and phenotypic cohort of Turkish consanguineous families characterized to date. We identified new candidate disease genes underlying the neurogenetic disorders, enabled provision of reproductive counselling and disease-specific therapies for some of the families, generated extended knowledge on genotype-phenotype relations in detail through systematic deep phenotyping, started functional studies for better understanding of the underlying molecular and cellular pathophysiology in neurogenetic conditions. We clearly showed that the higher mitochondrial etiology behind the cases which are initially diagnosed as pure neurological conditions. And most importantly, we established a detailed set of information on a large cohort of consanguineous Turkish families as the basis for future studies.

6. FUTURE PERSPECTIVES

Data from 3rd batch (51 families) will be available soon and data analysis will be carried out on RD-Connect Platform for identification of causal genes.

At the end of data analysis, unsolved families will be comprehensively analyzed by taking into account already identified SNVs, InDels, CNVs. Whole Genome Sequencing (WGS) and transcriptome analysis will be applied to identify variants affecting regulatory regions, structural variants, splicing variants and affected biological pathways through transcript expression levels.

Functional in vivo and in vitro studies for novel candidate genes and variants will be continued especially by putting great emphasis on mitochondrial group. New project entitled "Molecular pathways in rare, severe, early-onset neurogenetic disorders" will try to identify converging pathways essential for neuron function in novel genes by using neuronal progenitor cells (iNPCs) derived from primary patient fibroblasts, CRISPR/Cas9 mediated zebrafish models and multi-omic analyses.

7. REFERENCES

Abdulhag, U. N., Soiferman, D., Schueler-furman, O., Miller, C., Shaag, A., Elpeleg, O., … Saada, A. (2014). Mitochondrial complex IV deficiency , caused by mutated COX6B1 , is associated with encephalomyopathy , hydrocephalus and cardiomyopathy, *23*(2), 159–164. https://doi.org/10.1038/ejhg.2014.85

Adzhubei, I. A., Schmidt, S., Peshkin, L., Ramensky, V. E., Gerasimova, A., Bork, P., … Sunyaev, S. R. (2010). A method and server for predicting damaging missense mutations. *Nature Methods*, *7*(4), 248–249. https://doi.org/10.1038/nmeth0410-248

Alston, C. L., Rocha, M. C., Lax, N. Z., Turnbull, D. M., & Taylor, R. W. (2017). The genetics and pathology of mitochondrial disease. *Journal of Pathology*, *241*(2), 236–250. https://doi.org/10.1002/path.4809

Altshuler, D., Daly, M. J., & Lander, E. S. (2008). Genetic Mapping in Human Disease. *Science*, *322*(5903), 881 LP – 888. https://doi.org/10.1126/science.1156409

Ardissone, A., Invernizzi, F., Nasca, A., Moroni, I., Farina, L., & Ghezzi, D. (2015). Mitochondrial leukoencephalopathy and complex II deficiency associated with a recessive SDHB mutation with reduced penetrance. *Molecular Genetics and Metabolism Reports*, *5*, 51–54. https://doi.org/10.1016/j.ymgmr.2015.10.006

Balci, B., Uyanik, G., Dincer, P., Gross, C., Willer, T., Talim, B., … Topaloğlu, H. (2005). An autosomal recessive limb girdle muscular dystrophy (LGMD2) with mild mental retardation is allelic to Walker-Warburg syndrome (WWS) caused by a mutation in the POMT1 gene. *Neuromuscular Disorders*, *15*(4), 271–275. https://doi.org/10.1016/j.nmd.2005.01.013

Bao, R., Huang, L., Andrade, J., Tan, W., Kibbe, W. A., Jiang, H., & Feng, G. (2014). Review of Current Methods, Applications, and Data Management for the Bioinformatics Analysis of Whole Exome Sequencing, *13*, 67–82. https://doi.org/10.4137/CIN.S13779.Received

Barba, M., Czosnek, H., & Hadidi, A. (2014). Historical Perspective, Development and Applications of Next-Generation Sequencing in Plant Virology. *Viruses*, *6*, 106–136. https://doi.org/10.3390/v6010106

Bénit, P., Lebon, S., & Rustin, P. (2008). Respiratory-chain diseases related to complex III deficiency Biochimica et Biophysica Acta Respiratory-chain diseases related to complex III de fi ciency. *BBA - Molecular Cell Research*, *1793*(1), 181–185.

https://doi.org/10.1016/j.bbamcr.2008.06.004

Bezawork-Geleta, A., Rohlena, J., Dong, L., Pacak, K., & Neuzil, J. (2017). Mitochondrial Complex II: At the Crossroads. *Trends in Biochemical Sciences*, *42*(4), 312–325. https://doi.org/10.1016/j.tibs.2017.01.003

Biesecker, L. G., Shianna, K. V, & Mullikin, J. C. (2011). Exome sequencing: the expert view. *Genome Biology*, *12*(128), 12–14. https://doi.org/10.1186/gb-2011-12-9-128

Bird, T. D. (2005). Neurogenetic Diseases. *Trends in Pharmacological Sciences*, *22*, 126–128. https://doi.org/10.1016/s0165-6147(01)80057-2

Bittles, A. H., & Black, M. L. (2010). Consanguinity, human evolution, and complex diseases. *Proceedings of the National Academy of Sciences*, *107*(suppl_1), 1779–1786. https://doi.org/10.1073/pnas.0906079106

Choi, M., Scholl, U. I., Ji, W., Liu, T., Tikhonova, I. R., Zumbo, P., … Lifton, R. P. (2009). Genetic diagnosis by whole exome capture and massively parallel DNA sequencing.

Cingolani, P., Platts, A., Wang, L. L., Coon, M., Nguyen, T., Wang, L., … Ruden, D. M. (2012). A program for annotating and predicting the effects of single nucleotide polymorphisms, SnpEff: SNPs in the genome of Drosophila melanogaster strain w1118; iso-2; iso-3. *Fly (Austin)*, *6*(2), 80–92.

Dinh, T. A., Rosner, B. I., Atwood, J. C., Boland, C. R., Syngal, S., Vasen, H. F. A., … Burt, R. W. (2011). Health Benefits and Cost-Effectiveness of Primary Genetic Screening for Lynch Syndrome in the General Population. *American Association for Cancer Research*, *4*(1), 9–23. https://doi.org/10.1158/1940-6207.CAPR-10-0262

Dong, C., Wei, P., Jian, X., Gibbs, R., Boerwinkle, E., Wang, K., & Liu, X. (2015). Comparison and integration of deleteriousness prediction methods for nonsynonymous SNVs in whole exome sequencing studies. *Human Molecular Genetics*, *24*(8), 2125–2137. https://doi.org/10.1093/hmg/ddu733

Erzurumluoglu, A. M., Shihab, H. A., Rodriguez, S., Gaunt, T. R., & Day, I. N. M. (2016). Importance of Genetic Studies in Consanguineous Populations for the Characterization of Novel Human Gene Functions. *Annals of Human Genetics*, *80*(3), 187–196. https://doi.org/10.1111/ahg.12150

Eubel, H., Braun, H. P., & Millar, A. H. (2005). Blue-native PAGE in plants: A tool in analysis of protein-protein interactions. *Plant Methods*, *1*(1), 1–13. https://doi.org/10.1186/1746-4811-1-11

Faghihi, M. A., Mottagui-Tabar, S., & Wahlestedt, C. (2004). Genetics of neurological disorders. *Expert Review of Molecular Diagnostics*, *4*(3), 317. https://doi.org/10.1586/14737159.4.3.317

Fassone, E., & Rahman, S. (2012). Complex I de fi ciency : clinical features , biochemistry and molecular genetics, 578–590. https://doi.org/10.1136/jmedgenet-2012-101159

Fernández-Vizarra, E., & Zeviani, M. (2015). Nuclear gene mutations as the cause of mitochondrial complex III deficiency. *Frontiers in Genetics*, *6*(APR), 1–11. https://doi.org/10.3389/fgene.2015.00134

Fogel, B. L., Satya-Murti, S., & Cohen, B. H. (2016). Clinical exome sequencing in neurologic disease: AAN model coverage policy. *Neurology: Clinical Practice*, *6*(4), 368–368. https://doi.org/10.1212/cpj.0000000000000277

Foo, J., Liu, J., & Tan, E. (2012). Whole-genome and whole-exome sequencing in neurological diseases. *Nature Publishing Group*, *8*(9), 508–517. https://doi.org/10.1038/nrneurol.2012.148

Formosa, L. E., Dibley, M. G., Stroud, D. A., & Ryan, M. T. (2018). Building a complex complex: Assembly of mitochondrial respiratory chain complex I. *Seminars in Cell and Developmental Biology*, *76*, 154–162. https://doi.org/10.1016/j.semcdb.2017.08.011

Giachin, G., Bouverot, R., Acajjaoui, S., & Pantalone, S. (2016). Dynamics of Human Mitochondrial Complex I Assembly : Implications for Neurodegenerative Diseases, *3*(August), 1–20. https://doi.org/10.3389/fmolb.2016.00043

Girdea, M., Dumitriu, S., Fiume, M., Bowdin, S., Boycott, K. M., Chitayat, D., … Brudno, M. (2013). PhenoTips : Patient Phenotyping Software for Clinical and Research Use. https://doi.org/10.1002/humu.22347

Gradishar, W., Johnson, K., Brown, K., Mundt, E., & Manley, S. (2017). Clinical Variant Classification : A Comparison of Public Databases and a Commercial Testing Laboratory. *The Oncologist*, *22*(7), 797–803.

Gray, M. W. (2012). Mitochondrial Evolution. *Cold Spring Harbor Perspectives in Biology*, *4*(9), a011403–a011403.

Günther, K., Wörsdörfer, P., Meyer, S., Edenhofer, F., & Thier, M. (2015). Derivation of Adult Human Fibroblasts and their Direct Conversion into Expandable Neural Progenitor Cells. *Journal of Visualized Experiments*, (101), 1–10. https://doi.org/10.3791/52831

Gusella JF, Wexler NS, Conneally PM, Naylor SL, Anderson MA, Tanzi RE, Watkins PC,

Ottina K, Wallace MR, S. A. (1983). A polymorphic DNA marker genetically linked to Huntington's disease. *Nature*, *306*(5940), 234–238. https://doi.org/10.1038/306234a0

Hamamy, H. (2012). Consanguineous marriages preconception consultation in primary health care settings. *Journal of Community Genetics*, *3*(3), 185–192. https://doi.org/10.1007/s12687-011-0072-y

Huang Y, Yu S, Wu Z, T. B. (2014). Genetics of hereditary neurological disorders in children. *Transl Pediatr. , 3*(2), 108–119. https://doi.org/10.3978/j.issn.2224-4336.2014.03.04

Hunt, S. E., Mclaren, W., Gil, L., Thormann, A., Schuilenburg, H., Sheppard, D., … Cunningham, F. (2018). Ensembl variation resources. *Database*, *2018*, 1–13. https://doi.org/10.1093/database/bay119

Jackson, M., Marks, L., May, G. H. W., & Wilson, J. B. (2018). The genetic basis of disease. *Essays in Biochemistry*, *62*(October), 643–723.

Johns, M. B., & Paulus-Thomas, J. E. (1989). Purification of human genomic DNA from whole blood using sodium perchlorate in place of phenol. *Analytical Biochemistry*, *180*(2), 276–278. https://doi.org/10.1016/0003-2697(89)90430-2

Jonckheere, A. I., & Smeitink, J. A. M. (2012). Mitochondrial ATP synthase : architecture , function and pathology, 211–225. https://doi.org/10.1007/s10545-011-9382-9

Kaplan, S., Pinar, G., Kaplan, B., Aslantekin, F., Karabulut, E., Ayar, B., & Dilmen, U. (2016). The Prevalence of Consanguineous Marriages and Affecting Factors in Turkey: a National Survey. *Journal of Biosocial Science*, *48*(5), 616–630. https://doi.org/10.1017/s0021932016000055

Keogh, M. J., & Chinnery, P. F. (2013). Next generation sequencing for neurological diseases : New hope or new hype ? *Clinical Neurology and Neurosurgery*, *115*(7), 948–953. https://doi.org/10.1016/j.clineuro.2012.09.030

Khalid, R., & Ahmad, S. (2016). Principle, Analysis, Application and Challenges of Next-Generation Sequencing: A Review. *ArXiv Preprint Ar-Xiv:160605254*.

Koht, J., Stevanin, G., Durr, A., Mundwiller, E., Brice, A., & Tallaksen, C. M. E. (2012). SCA14 in Norway, two families with autosomal dominant cerebellar ataxia and a novel mutation in the PRKCG gene. *Acta Neurologica Scandinavica*, *125*(2), 116–122. https://doi.org/10.1111/j.1600-0404.2011.01504.x

Kumar, A. (2016). Mitochondrial Dysfunction & Neurological Disorders. *Current Neuropharmacology*, *14*(6), 565–566.

Lee, H., Gurtowski, J., Yoo, S., Nattestad, M., Marcus, S., Goodwin, S., … Schatz, M. C. (2016). Third-generation sequencing and the future of genomics, (Table 1).

Loeffen, J. L. C. M., Smeitink, J. A. M., Trijbels, J. M. F., Janssen, A. J. M., & Triepels, R. H. (2000). Isolated Complex I Deficiency in Children : Clinical , Biochemical and Genetic Aspects, *134*.

McKenzie, M., Thorburn, D. R., Lazarou, M., Smith, S. M., & Ryan, M. T. (2009). Assembly of nuclear DNA-encoded subunits into mitochondrial complex IV, and their preferential integration into supercomplex forms in patient mitochondria. *FEBS Journal*, *276*(22), 6701–6713. https://doi.org/10.1111/j.1742-4658.2009.07384.x

Menon, R. K., Trucco, M., Stratakis, C. A., & Sci, D. (2014). *Molecular Endocrinology and Endocrine Genetics*. *PEDIATRIC ENDOCRINOLOGY* (FOURTH EDI). Elsevier Inc. https://doi.org/10.1016/B978-1-4557-4858-7.00011-1

Mimaki, M., Wang, X., Mckenzie, M., Thorburn, D. R., & Ryan, M. T. (2012). Biochimica et Biophysica Acta Understanding mitochondrial complex I assembly in health and disease ☆. *BBA - Bioenergetics*, *1817*(6), 851–862. https://doi.org/10.1016/j.bbabio.2011.08.010

Niemi, N. M., Lanning, N. J., Westrate, L. M., & Mackeigan, J. P. (2013). Downregulation of the Mitochondrial Phosphatase PTPMT1 Is Sufficient to Promote Cancer Cell Death. *PLoS ONE*, *8*(1). https://doi.org/10.1371/journal.pone.0053803

Park, S. T. (2016). Trends in Next-Generation Sequencing and a New Era for Whole Genome Sequencing. *International Neurourology Journal*, *20*(Suppl 2), S76-83.

Pendergrass, W., Wolf, N., & Poot, M. (2004). Efficacy of MitoTracker Green ™ and CMXRosamine to Measure Changes in Mitochondrial Membrane Potentials in Living Cells and Tissues. *Cytometry A*, *61*(2), 162–169. https://doi.org/10.1002/cyto.a.20033

Pulst, S. M. (1999). Genetic Linkage Analysis. *Arch Neurol.*, *56*(6), 667–672.

Reijnders, M. R. F., Miller, K. A., Alvi, M., Goos, J. A. C., Lees, M. M., de Burca, A., … Wilkie, A. O. M. (2018). De Novo and Inherited Loss-of-Function Variants in TLK2: Clinical and Genotype-Phenotype Evaluation of a Distinct Neurodevelopmental Disorder. *American Journal of Human Genetics*, *102*(6), 1195–1203. https://doi.org/10.1016/j.ajhg.2018.04.014

Rentzsch, P., Witten, D., Cooper, G. M., Shendure, J., & Kircher, M. (2019). CADD: Predicting the deleteriousness of variants throughout the human genome. *Nucleic Acids Research*, *47*(D1), D886–D894. https://doi.org/10.1093/nar/gky1016

Robinson, P. N., Piro, R. M., & Jäger, M. (2017). *Computational Exome and Genome Analysis*. Retrieved from https://books.google.com.tr/books?id=fmpQDwAAQBAJ&dq=unsolved+cases+after+wes&source=gbs_navlinks_s

Sarıkaya, E. (2018). TÜRKİYE ANNE, ÇOCUK VE ERGEN SAĞLIĞI ENSTİTÜSÜ NADİR HASTALIKLAR FARKINDALIK GÜNÜ TOPLANTISI SUNUM KİTAPÇIĞI. Retrieved from http://www.tuseb.gov.tr/tacese

Schaffer, A. E., Eggens, V. R. C., Caglayan, A. O., Reuter, M. S., Scott, E., Coufal, N. G., … Gleeson, J. G. (2014). CLP1 founder mutation links tRNA splicing and maturation to cerebellar development and neurodegeneration. *Cell*, *157*(3), 651–663. https://doi.org/10.1016/j.cell.2014.03.049

Schwartz, T. S., Wojcik, M. H., Pelletier, R. C., Edward, H. L., Picker, J. D., Holm, I. A., … Pankaj, B. (2018). Short Title : Expanding the Phenotypic Spectrum of OPHN1. *European Journal of Medical Genetics*. https://doi.org/10.1016/j.ejmg.2018.06.015

Schwarz, J. M., Cooper, D. N., Schuelke, M., & Seelow, D. (2014). MutationTaster2 : mutation prediction for the deep-sequencing age. *Nature Publishing Group*, *11*(4), 361–362. https://doi.org/10.1038/nmeth.2890

Signes, A., & Fernandez-vizarra, E. (2018). Assembly of mammalian oxidative phosphorylation complexes I – V and supercomplexes. *Essays in Biochemistry*, *62*, 255–270.

Signes, A., & Fernandez-Vizarra, E. (2018). Assembly of mammalian oxidative phosphorylation complexes I–V and supercomplexes. *Essays In Biochemistry*, *62*(3), 255–270. https://doi.org/10.1042/ebc20170098

Sim, N. L., Kumar, P., Hu, J., Henikoff, S., Schneider, G., & Ng, P. C. (2012). SIFT web server: Predicting effects of amino acid substitutions on proteins. *Nucleic Acids Research*, *40*(W1), 452–457. https://doi.org/10.1093/nar/gks539

Sims, D., Sudbery, I., Ilott, N. E., Heger, A., & Ponting, C. P. (2014). Sequencing depth and coverage : key considerations in genomic analyses. *Nature Publishing Group*, *15*(2), 121–132. https://doi.org/10.1038/nrg3642

Smeitink, J., Heuvel, L. Van Den, & Dimauro, S. (2001). THE GENETICS AND PATHOLOGY OF OXIDATIVE PHOSPHORYLATION, *2*(May), 342–352.

Stein, C., & Elston, R. (2009). Finding genes underlying human disease. *Clin Genet.*, *75*(2),

101–106. https://doi.org/10.1038/mp.2011.182.doi

Stroud, D. A., Ryan, M. T., Surgenor, E. E., Frazier, A. E., Beilharz, T. H., Thorburn, D. R., … Stait, T. (2016). Accessory subunits are integral for assembly and function of human mitochondrial complex I. *Nature*, *538*(7623), 123–126. https://doi.org/10.1038/nature19754

Tetreault, M., Bareke, E., Nadaf, J., Alirezaie, N., & Majewski, J. (2015). Whole-exome sequencing as a diagnostic tool: Current challenges and future opportunities. *Expert Review of Molecular Diagnostics*, *15*(6), 749–760. https://doi.org/10.1586/14737159.2015.1039516

Thompson, R., Chem, M., Johnston, L., Ph, D., Taruscio, D., Ph, D., … Ph, D. (2014). RD-Connect : An Integrated Platform Connecting Databases , Registries , Biobanks and Clinical Bioinformatics for Rare Disease. *Journal of General Internal Medicine*, *29*, 780–787. https://doi.org/10.1007/s11606-014-2908-8

Toft, M. (2014). Advances in genetic diagnosis of neurological disorders. *Acta Neurologica Scandinavica*, *129*(S198), 20–25. https://doi.org/10.1111/ane.12232

Trujillano, D., Bertoli-Avella, A. M., Kumar Kandaswamy, K., Weiss, M. E., Köster, J., Marais, A., … Abou Jamra, R. (2017). Clinical exome sequencing: Results from 2819 samples reflecting 1000 families. *European Journal of Human Genetics*, *25*(2), 176–182. https://doi.org/10.1038/ejhg.2016.146

Van De Warrenburg, B. P. C., Verbeek, D. S., Piersma, S. J., Hennekam, F. A. M., Pearson, P. L., Knoers, N. V. A. M., … Sinke, R. J. (2003). Identification of a novel SCA14 mutation in a Dutch autosomal dominant cerebellar ataxia family. *Neurology*, *61*(12), 1760–1765. https://doi.org/10.1212/01.WNL.0000098883.79421.73

Variants, alleles and haplotypes | EMBL-EBI Train online. (n.d.). Retrieved May 26, 2019, from https://www.ebi.ac.uk/training/online/course/human-genetic-variation-introduction/what-genetic-variation/types-genetic-variation/variants

Weely, W. S. Van, Ph, D., Leufkens, P. H. G. M., Vrueh, B. R. De, Ph, D., Baekelandt, E. R. F., & Haan, J. M. H. De. (2013). Priority Medicines for Europe and the World " A Public Health Approach to Innovation " Update on 2004 Background Paper Background Paper 6 . 19 Rare Diseases, (March).

Williams, K. L. (2018). Gene Mapping. *Encyclopedia of Bioinformatics and Computational Biology*, *2*, 242–250. https://doi.org/10.1016/B978-0-12-809633-8.20233-1

Yabe, I., Kimura, M., Shirai, S., Takahashi, I., Matsushima, M., & Sasaki, H. (2016). Spinocerebellar ataxia type 14 family with a novel PRKCG mutation . *Neurology and Clinical Neuroscience*, *4*(5), 199–200. https://doi.org/10.1111/ncn3.12070

Zhang, J., Guan, Z., Murphy, A. N., Wiley, S. E., Perkins, G. A., Worby, C. A., … Dixon, J. E. (2011). Mitochondrial phosphatase PTPMT1 is essential for cardiolipin biosynthesis. *Cell Metabolism*, *13*(6), 690–700. https://doi.org/10.1016/j.cmet.2011.04.007

Zheng, H., Yu, W., Shen, J., Kang, S., Hambardzumyan, D., Li, J. Y., … Qu, C. (2018). Mitochondrial oxidation of the carbohydrate fuel is required for neural precursor / stem cell function and postnatal cerebellar development. *Science Advances*, *4*(10), 1–14.

8. APPENDIX

Research Ethics Committee Approval

KLİNİK ARAŞTIRMALAR ETİK KURULU KARAR FORMU

ARAŞTIRMANIN AÇIK ADI	Türkiye'de Akraba Evliliklerine Bağlı Nörogenetik Hastalık Yükünün Araştırılmasına Yeni Genomik Yaklaşımlar
VARSA ARAŞTIRMANIN PROTOKOL KODU	-
ETİK KURUL PROTOKOL NUMARASI	302-SBKAEK

ETİK KURUL BİLGİLERİ	ETİK KURULUN ADI	Dokuz Eylül Üniversitesi Klinik Araştırmalar Etik Kurulu
	AÇIK ADRESİ:	Dokuz Eylül Üniversitesi Sağlık Yerleşkesi Dekanlık Binası Kat:2 İnciraltı 35340 İZMİR-TÜRKİYE
	TELEFON	0 232 4122254 - 0 232 4122258
	FAKS	0232 4122243
	E-POSTA	etikkurul@deu.edu.tr

BAŞVURU BİLGİLERİ	KOORDİNATÖR/SORUMLU ARAŞTIRMACI UNVANI/ADI/SOYADI	Prof.Dr.Semra HIZ			
	KOORDİNATÖR/SORUMLU ARAŞTIRMACININ UZMANLIK ALANI	Nöroloji			
	KOORDİNATÖR/SORUMLU ARAŞTIRMACININ BULUNDUĞU MERKEZ	Dokuz Eylül Üniversitesi Çocuk Nöroloji A.D			
	VARSA İDARİ SORUMLU UNVANI/ADI/SOYADI	-			
	DESTEKLEYİCİ				
	PROJE YÜRÜTÜCÜSÜ UNVANI/ADI/SOYADI (TÜBİTAK vb. gibi kaynaklardan destek alanlar için)				
	DESTEKLEYİCİNİN YASAL TEMSİLCİSİ				
	ARAŞTIRMANIN FAZI VE TÜRÜ	FAZ 1	☐		
		FAZ 2	☐		
		FAZ 3	☐		
		FAZ 4	☐		
		Gözlemsel ilaç çalışması	☐		
		Tıbbi cihaz klinik araştırması	☐		
		İn vitro tıbbi tanı cihazları ile yapılan performans değerlendirme çalışmaları	☐		
		İlaç dışı klinik araştırma	☒		
		Diğer ise belirtiniz			
	ARAŞTIRMAYA KATILAN MERKEZLER	TEK MERKEZ ☒	ÇOK MERKEZLİ ☐	ULUSAL ☒	ULUSLARARASI ☐

	Belge Adı	Tarihi	Versiyon Numarası	Dili		
DEĞERLENDİRİLEN BELGELER	ARAŞTIRMA PROTOKOLÜ	mevcut		Türkçe ☐	İngilizce ☐	Diğer ☐
	Bilgilendirilmiş Gönüllü Olur Formu	mevcut		Türkçe ☐	İngilizce ☐	Diğer ☐
	OLGU RAPOR FORMU	mevcut		Türkçe ☐	İngilizce ☐	Diğer ☐
	ARAŞTIRMA BROŞÜRÜ			Türkçe ☐	İngilizce ☐	Diğer ☐
DEĞERLENDİRİLEN DİĞER BELGELER	Belge Adı			Açıklama		
	SİGORTA	☐				
	ARAŞTIRMA BÜTÇESİ	☐		Mevcut 28.01.2016		
	BİYOLOJİK MATERYEL TRANSFER FORMU	☐				
	İLAN	☐				
	YILLIK BİLDİRİM	☐				
	SONUÇ RAPORU	☐				
	GÜVENLİLİK BİLDİRİMLERİ	☐				
	DİĞER:	☐		-Araştırma akış şeması -Biyolojik Materyal Transfer Formu 29.01.2016 tarihli imzalı -Araştırmacı özgeçmişleri		

Etik Kurul Başkanının
Unvanı/Adı/Soyadı: Prof.Dr.Ayşegül Yıldız
İmza:

Mukaddes AKKECE
Enstitü Sekreteri

Not: Etik kurul başkanı, imzasının yer almadığı her sayfaya imza atmalıdır.

KLİNİK ARAŞTIRMALAR ETİK KURULU KARAR FORMU

ARAŞTIRMANIN AÇIK ADI	Türkiye'de Akraba Evliliklerine Bağlı Nörogenetik Hastalık Yükünün Araştırılmasına Yeni Genomik Yaklaşımlar
VARSA ARAŞTIRMANIN PROTOKOL KODU	-
ETİK KURUL PROTOKOL NUMARASI	302-SBKAEK

KARAR BİLGİLERİ	Karar No:2016/03-01	Tarih:11.02.2016
	Yukarıda bilgileri verilen başvuru dosyası ile ilgili belgeler araştırmanın/çalışmanın gerekçe, amaç, yaklaşım ve yöntemleri dikkate alınarak incelenmiş ve uygun bulunmuş olup araştırmanın/çalışmanın başvuru dosyasında belirtilen merkezlerde gerçekleştirilmesinde etik ve bilimsel sakınca bulunmadığına toplantıya katılan etik kurul üye tam sayısının salt çoğunluğu ile karar verilmiştir.	

KLİNİK ARAŞTIRMALAR ETİK KURULU	
ETİK KURULUN ÇALIŞMA ESASI	İlaç ve Biyolojik Ürünlerin Klinik Araştırmaları Hakkında Yönetmelik, İyi Klinik Uygulamaları Kılavuzu
BAŞKANIN UNVANI / ADI / SOYADI:	Prof.Dr.Ayşegül Yıldız

Unvanı/Adı/Soyadı	Uzmanlık Alanı	Kurumu	Cinsiyet		Araştırma ile ilişki		Katılım *		İmza
Prof.Dr.Ayşegül YILDIZ	Psikiyatri	DEU Tıp Fakültesi Psikiyatri Anabilim Dalı	E ☐	K ☒	E ☐	H ☒	E ☐	H ☐	
Prof.Dr.Hülya ELLİDOKUZ	Halk Sağlığı	DEU Onkoloji Enstitüsü Prevantif Onkoloji A.D.	E ☐	K ☒	E ☐	H ☒	E ☐	H ☐	
Prof.Dr.Nuray DUMAN	Çocuk Sağlığı ve Hastalıkları (Yeni Doğan)	DEU Tıp Fakültesi Çocuk Sağlığı ve Hastalıkları Anabilim Dalı	E ☐	K ☒	E ☐	H ☒	E ☐	H ☐	
Prof.Dr.Hale ÖREN	Çocuk Sağlığı ve Hastalıkları (Çocuk Hematoloji)	DEU Tıp Fakültesi Çocuk Sağlığı ve Hastalıkları Anabilim Dalı	E ☐	K ☒	E ☐	H ☒	E ☐	H ☐	
Prof.Dr.A.Necati GÖKMEN	Anesteziyoloji ve Reanimasyon	Anesteziyoloji ve Reanimasyon A.D	E ☒	K ☐	E ☐	H ☒	E ☐	H ☐	
Prof.Dr.Taner DAĞCI	Fizyoloji	Ege Üniversitesi Tıp Fakültesi	E ☒	K ☐	E ☐	H ☒	E ☐	H ☐	
Doç.Dr.Pembe KESKİNOĞLU	Biyoistatistik	DEU Tıp Fakültesi Biyoistatistik ve Tıbbi Bilişim A.D	E ☐	K ☒	E ☐	H ☒	E ☐	H ☐	
Doç.Dr.Erdem YAKA	Nöroloji	DEU Tıp Fakültesi Nöroloji A.D	E ☒	K ☐	E ☐	H ☒	E ☐	H ☐	
Doç.Dr.Uğur Önsel TÜRK	Kardiyoloji	Ege Üniversitesi İlaç ve Farmakokinetik Arş-Uyg.Merk	E ☒	K ☐	E ☐	H ☒	E ☐	H ☐	
Doç.Dr.Yasemin BAŞKIN	Temel Onkoloji	DEU Onkoloji Enstitüsü Temel Onkoloji A.D	E ☐	K ☒	E ☐	H ☒	E ☐	H ☐	
Yard.Doç.Dr.Yasemin ERAÇ	Farmakoloji	Ege Üniversitesi Eczacılık Fakültesi Farmakoloji Anabilim Dalı	E ☐	K ☒	E ☐	H ☒	E ☐	H ☐	
Av.Semra MARMARA	Hukuk	DEÜ Rektörlüğü	E ☐	K ☒	E ☐	H ☒	E ☐	H ☐	
Av.Nazan PEDÜKCOŞKUN	Hukuk	Alsancak Nevvar Salih İşgören Hastanesi	E ☐	K ☒	E ☐	H ☒	E ☐	H ☐	
Hayat ALBAYRAK	Emekli	Sağlık Mesleği Mensubu Olmayan Üye	E ☐	K ☒	E ☐	H ☒	E ☐	H ☐	

*:Toplantıda Bulunma

Etik Kurul Başkanının
Unvanı/Adı/Soyadı: Prof.Dr.Ayşegül Yıldız
İmza:

Mukaddes AKKEÇELİ
Enstitü Sekreteri

Not: Etik kurul başkanı, imzasının yer almadığı her sayfaya imza atmalıdır.